PASSIVE Q-SWITCHED FIBER LASER IN C- AND S-BAND REGION USING SILVER NANOPARTICLES AS A SATURABLE ABSORBER

NUR E'ZZATI BINTI RUSLAN

INSTITUTE FOR ADVANCED STUDIES
UNIVERSITY OF MALAYA
KUALA LUMPUR

2019

PASSIVE Q-SWITCHED FIBER LASER IN C- AND S-BAND REGION USING SILVER NANOPARTICLES AS A SATURABLE ABSORBER

NUR E'ZZATI BINTI RUSLAN

DISSERTATION SUBMITTED IN FULFILMENT OF THE REQUIREMENTS FOR THE DEGREE OF MASTER OF PHILOSOPHY

**INSTITUTE FOR ADVANCED STUDIES
UNIVERSITY OF MALAYA
KUALA LUMPUR**

2019

UNIVERSITY OF MALAYA

ORIGINAL LITERARY WORK DECLARATION

Name of Candidate: Nur E'zzati binti Ruslan

Matric No: HGG 150002

Name of Degree:

Title of Project Paper/Research Report/Dissertation/Thesis ("this Work"):

Passive Q-switched Fiber Laser in C- and S-Band Region Using Silver Nanoparticles as Saturable Absorber

Field of Study: Photonic Science

I do solemnly and sincerely declare that:

(1) I am the sole author/writer of this Work;
(2) This Work is original;
(3) Any use of any work in which copyright exists was done by way of fair dealing and for permitted purposes and any excerpt or extract from, or reference to or reproduction of any copyright work has been disclosed expressly and sufficiently and the title of the Work and its authorship have been acknowledged in this Work;
(4) I do not have any actual knowledge nor do I ought reasonably to know that the making of this work constitutes an infringement of any copyright work;
(5) I hereby assign all and every rights in the copyright to this Work to the University of Malaya ("UM"), who henceforth shall be owner of the copyright in this Work and that any reproduction or use in any form or by any means whatsoever is prohibited without the written consent of UM having been first had and obtained;
(6) I am fully aware that if in the course of making this Work I have infringed any copyright whether intentionally or otherwise, I may be subject to legal action or any other action as may be determined by UM.

Candidate's Signature Date:

Subscribed and solemnly declared before,

Witness's Signature Date:

Name:

Designation:

PASSIVE Q-SWITCHED FIBER LASER IN C- AND S- BAND REGION USING SILVER-NANOPARTICLES AS SATURABLE ABSORBER

ABSTRACT

This research aims to investigate the feasibility of silver-nanoparticles as a saturable absorber (SA) to passively generate Q-switched pulses in C- and S- bands. Previously, passive Q-switched lasers is generated by employing nonlinear polarization rotation (NPR) and semiconductor saturable absorber mirrors (SESAMs). Recently, passive Q-switched lasers can also be generated using 2D materials such as single-walled carbon nanotubes (SWCNT), graphene and transition metal dichalcogenides. The performance of silver-nanoparticles saturable absorber will be investigated at C- and S- band regions. Silver-nanoparticles saturable absorber was made into thin film to allow for easy integration into fiber laser cavity. The measured modulation depth and saturation intensity of the silver-nanoparticle SA are 31.6% and 0.54 MW/cm2, respectively. When inserted between fiber ferrules, the silver-nanoparticles SA generated a self-starting passive Q-switched lasers operating in C- and S-bands. C-band Q-switched fiber laser has an increasing repetition rate from 19.4 – 74.1 kHz, while the pulsewidth decreased from 8.88 – 3.2 μs as pump power was increased. The laser also showed wavelength tunability from 1552.9 – 1580.2 nm. The repetition rate increased from 29 – 48 kHz, while the pulsewith decreased from 6.8 – 0.8 μs. The wavelength can be tuned from 1493nm to 1500nm. These results demonstrated that silver-nanoparticles is a new 2D material that can be utilized to generate passive Q-switched which can be utilized in various photonic application.

Keywords: Erbium-Doped Fiber , fiber laser, Q-switched laser, silver-nanoparticles

LASER GENTIAN OPTIK Q-SUIS PASIF DI KAWASAN JALUR C- DAN S- MENGGUNAKAN NANOPARTIKEL PERAK SEBAGAI PENYERAP TEPUAN

ABSTRAK

Kajian ini bertujuan untuk mengkaji kemungkinan nanopartikel perak sebagai penyerap tepuan(SA) untuk menjana denyutan Q-suis pasif di dalam jalur C- dan S-. Sebelum ini, laser Q-suis pasif telah dihasilkan menggunakan putaran linear polarisasi (NPR) dan penyerap tepuan semikonduktor cermin (SESAMs). Baru-baru ini, laser Q-suis pasif juga boleh dihasilkan menggunakan bahan-bahan 2D seperti nanotube tunggal berdinding karbon (SWCNT), grafit dan logam peralihan dikalkogenida. Prestasi nanopartikel perak sebagai penyerap tepuan disiasat di jalur C- dan S-. Nanopartikel perak SA telah dibuat dalam bentuk filem nipis untuk dimasukkan dengan mudah ke dalam rongga laser gentian optik. Kedalaman modulasi dan intensiti ketepuan nanopartikel perak SA adalah 31.6% dan 0.54 MW/cm^2. Apabila nanopartikel perak SA dimasukkan antara ferul fiber, nanopartikel perak SA menjana laser Q-suis pasif yang bermula dengan sendiri iaitu beroperasi di jalur C- dan S-. Laser gentian optic Q-suis di jalur C yang mempunyai kadar pengulangan meningkat dari 19.4-74.1 kHz, manakala lebar denyutan menurun dari 8.88-3.2 μs apabila kuasa pam dinaikkan. Laser itu juga menunjukkan panjang gelombang daya talaan dari 1552.9-1580.2 nm. Kadar pengulangan meningkat dari 29-48 kHz, manakala lebar-denyut semakin menurun dari 6.8-0.8 μs. Keputusan ini menunjukkan bahawa nanopartikel perak adalah bahan 2D baru yang boleh digunakan untuk menjana fiber gentian optic Q-suis pasif yang boleh digunakan di dalam pelbagai aplikasi fotonik.

Kata kunci :Erbium didopkan, fiber laser dan Q-suis laser dan nanopartikel perak

ACKNOWLEDGEMENTS

Alhamdullilah, would like to express my gratitude to The Almighty God for giving me the strength to complete this dissertation. In addition, my sincere thanks to all people that had helped me along this journey to complete my research works.

Foremost, my humble thanks to my beloved supervisor, Prof Harith bin Ahmad and also Dr Mohd Afiq bin Ismail. Without their supervision, motivation, enthusiasm, knowledge and support, I would be lost in the middle of my research. Again, thanks a lot give me guidance in completing my research for my masters study.

Next, it would go amiss if I did not convey my gratitude to my friends especially Pn Siti Aisyah and Ms Cherrie at Photonic Research centre(PRC) that always support, give motivation, ideas, suggestion and helpful assistance in order to finish my research works.

Last but not least, special thanks goes to my family, especially my husband, mother and father for their motivation and financial support from beginning until the end of my studies.

TABLE OF CONTENTS

LIST OF FIGURES

LIST OF TABLES

LIST OF ABBREVIATIONS

ASE	:	Amplified Spontaneous Emission
BP	:	Black Phosphorus
CNT	:	Saturable Absorber
DC-EDF	:	Depressed-Cladding Erbium-Doped Fiber
EDF	:	Erbium-Doped Fiber
MTMS	:	Methyltrimethoxylane
OSA	:	Optical Spectrum Analyzer
OPM	:	Optical Power Meter
SNPs	:	Silver-Nanoparticles
SA	:	Saturable Absorber
SESAM	:	Semiconductor Saturable Absorber Mirror
TMDs	:	Transition Metal Dichalcogenides
TBPF	:	Tunable Band-Pass Filter
TI	:	Topological Insulator

CHAPTER 1: INTRODUCTION

1.1 Background

During 1960s, fiber optics field gained rapid development substantially focused on image transmission over a bundle of glass fiber (Kapany, 1967). At the beginning of the of discoveries of fiber, the fiber produces extremely high loss which up to 1000 dB/km from modern standard but after following recommendation by (Kao & Hockham, 1966), remarkable changes in the silica fiber which shows the reduction of losses to below 20 dB/km (Kapron, Keck, & Maurer, 1970). In 1979s, due advancement in fabrication technology produces more reduction of silica fibers to only 0.2 dB/km at 1.55μm wavelength region (Miya, Terunuma, Hosaka, & Miyashita, 1979). The discovery of low-loss silica fibers not only introduces to the fiber optic communications but also open up to new future application of nonlinear fiber optics field (Agrawal, 1997; L. Mollenauer, Gordon, Mamyshev, Kaminow, & Koch, 1997; Ramaswami, Sivarajan, & Sasaki, 2009) and also eventually led Charles K. Kao to Nobel Prize in Physic in 2009. Early 1972, scientist starts(Nikolaus & Grischkowsky, 1983) to explore optical fibers of Stimulated Raman and Brillouin-Scattering (Ippen & Stolen, 1972; Smith, 1972; R. H. Stolen, Ippen, & Tynes, 1972), optically produced parametric four-wave mixing, birefringence and self-phase modulation (Hill, Johnson, Kawasaki, & MacDonald, 1978; R. Stolen & Ashkin, 1973; R. Stolen, Bjorkholm, & Ashkin, 1974). The invention of optical soliton in 1980s has led to the formation of ultrashort optical pulses (Gordon & Haus, 1986; Gouveia-Neto, Gomes, & Taylor, 1988; Islam, Simpson, Shang, Mollenauer, & Stolen, 1987; Kafka & Baer, 1987; L. F. Mollenauer & Stolen, 1984) and increase number of research in pulse compression and optical switching methods which then exploited the nonlinear effect in the fibers (Nakatsuka, Grischkowsky, & Balant, 1981; Nikolaus & Grischkowsky, 1983; Shank, Fork, Yen, Stolen, & Tomlinson, 1982).

Nonlinear fiber optics field continue to blossom because highly demand in 1990s. Scientist has enhance the optical fibers with added rare-earth element to produce amplifier and lasers (Digonnet, 1993). Erbium-doped fiber amplifiers gained most attraction because their efficiency in amplify the light at 1.5µm wavelength region(C-band) and have the minimum loss. Due to data traffic of conventional wavelength, the newer transmission which is S-band (1400nm to 1530nm) is introduced. The S-band amplification is attained by suppressed the amplified spontaneous emission (ASE) in C-band region wavelength by implement the fundamental mode- cutoff of the depressed-cladding erbium-doped fiber (DC-EDF)(Chen, Chi, & Tseng, 2005; Yeh, Lee, & Chi, 2004).

The emergence of the Q-switched technology hold high advantages including high pulse energy and short pulse width that can be used in nonlinear optics(Geist et al., 1997; Stöppler, Kieleck, & Eichhorn, 2010), remote sensing, range finding, laser radar, biotechnology, spectroscopy and telecommunication(Kilpelä, Pennala, & Kostamovaara, 2001; Koechner, 2013; Kölbl, Fröschl, Seedsman, & Sperber, 2008; Stöppler et al., 2010). Q-switching allow the modulation of losses in laser resonator through active or passive method. Active method requires external powered equipment such as electro-optic (El-Sherif & King, 2003; Michelangeli, Giuliani, Palange, & Penco, 1986) and acoustic-optic modulators(Delgado-Pinar, Zalvidea, Diez, Pérez-Millán, & Andrés, 2006). Whereas for passively method using saturable absorber (SA) that more preferable due to easy integration into laser cavity system, high reliability and low cost.

Metal nanoparticles has blossomed over past decades due to its extraordinary optical properties. Metal nanoparticles plays important roles in serving as SA. Metal nanoparticles such as silver nanoparticles(SNPs) significant abilities which highly dispersed support to enhance the signal from organic molecules in Raman Spectroscopy application (Creighton, Blatchford, & Albrecht, 1979; Lee & Meisel, 1982) has attracted scientist attention to this material. The SNPs material show very excellent performance and the rapid progress has been made to this material which can be proved by increasing number of scientific journal dedicated to investigation of this material.

1.2 Research objectives and scope of research

This research work will focus on generation of Q-switched operation at S-band (1460-1530nm) and C-band (1530-1560nm) wavelengths by employing silver-nanoparticles as a SA. To achieve desire laser operation wavelengths, the Depressed Cladding Erbium-Doped Fiber (DC-EDF) and Erbium-Doped Fiber (EDF) as the gain medium and will be pumped by 974nm laser diode.

To generate the Q-switched operation, nonlinear properties of the SNPs thin-film will be measured such as the modulation depth and the saturation intensity of the silver-nanoparticles. The performances of Q-switched operation will be investigated by employing the SA based on the trends of repetition rate and pulse width, laser spectrum and the output power of the laser which are will be measured by Oscilloscope, Optical Spectrum Analyzer (OSA) and Optical Power Meter (OPM). This research includes the calculation and analyzing the experimental data. Then, the results will compare to the existing SA in term of pulsed laser system.

The objectives of this works are as follows:

a) To characterize the optical properties of Silver-nanoparticle film as saturaber absorber (SA), which includes the preparation of thin-film and nonlinear absorption properties of the SA.

b) To design the laser cavity of S- and C- bands region wavelength.

c) To generate and analyze passive Q switching operation at and S- and C- bands region wavelength, which emits short-pulsed laser (approximately from microsecond to nanosecond).

1.3 Dissertation Overview

This dissertation reports the introduction of the fiber, its working principle, the experimental set-up, collection of data and the discussion of the result which entitled Passively Q-switched Fiber Laser in wavelength region S- and C- bands using SNPs based SA. This dissertation consist of five chapters. The first chapter briefly describe the background of the fiber, objectives and as well as the scope of the researches.

Chapter two of this dissertation will cover some literature review about the laser, fiber optic and laser principles. This chapter also provide detail description on the level diagram of the gain medium and its working principles in laser application. Furthermore, the Q-switched techniques and the theory working principle of the SA as well as SNPs based SA to produce the passive Q-switched laser. Preparation of the SNPs and its nonlinear properties is describe in chapter three. Chapter four and five will be introduces to experimental method and result gathered from the generation of the Q-switched pulsed using SNPs thin film material as SA at S- and C- band region wavelength. Finally, chapter six will summarizes the dissertations with a few recommendation for further work.

CHAPTER 2: LITERATURE REVIEW

2.1 Background of laser and fiber optics

2.1.1 Laser

In 1958, the laser principles was discovered by Charles Townes and Arthur Schalow from Bell Telephone Laboratories(Schawlow & Townes, 1958). Since Theodore Maiman, who was then at Hughes Research Laboratories, demonstrated the first working laser, using a ruby crystal in 1960(Maiman, 1960), there has been a lot of different types of lasers invented by other researchers. But, only a few have found to be feasible applications in industrial, scientific, military and commercial applications. Among them are including helium neon laser (the first continuous-wave laser), air-cooled ion lasers and the semiconductor diode laser.

LASER or Light Amplification by Stimulated Emission of Radiation is high power, coherent, monochromatic and collimated. These properties are the one that differentiate between the laser and normal light, like the one from a light bulb. The beam of a laser has higher intensity than the beam of that a light bulb. Coherent indicate that the laser beams has a fixed phase relationship with each other. Highly collimated means laser has a low divergence. A laser can travel over long distances and at the same time, maintain a high light intensity. Monochromatic suggest that a laser emit at single wavelength. Figure 2.1 illustrates the difference between the light from a light bulb and a laser.

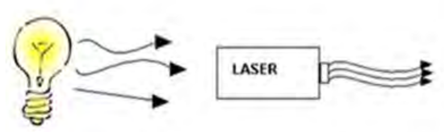

Figure 2. 1: The comparison between incoherent light bulb and coherent laser(Renk, 2012).

2.2 Fiber optic

Fiber optics is light transmission over a very fine glass or plastic fibers. Light travels in fibre optics by total internal refraction principle. The remarkable discovery in optical communication by Charles K. Kao and George A. Hockham from Standard Telecommunication Laboratories, U.K came in 1966(Kao & Hockham, 1966). Before their pioneering work, fiber glass was believed to have the potential to carry light. However, it was not suitable because of their excessively high loss of signal from Rayleigh scattering. In 1965, Kao and Hockham came out with theories for the fundamental limitation for glass. Using their finding, light attenuation was successfully reduced to 20dB/km. Previously, light attenuation in fiber optics was 1000dB/km. Upon after a few further investigations on the glass material, they had identified that the main problem lied in the impurities inside the material itself. Therefore, a new low-loss material was needed to tackle the problem. They experimented with various kinds of material and had identified fused-silica (SiO_2) as an excellent candidate.

Their remarkable discovery triggered a rapid development in various photonics application based on fiber optics. Their discovery eventually led to winning the Nobel Prize in Physics in 2009. Due to the increase in demand for data transmission, fiber optics has become the new alternative to replace the existing copper cables. The advantages of fiber optic compare to copper carbles are;

i.) fiber optics has high signal bandwidth (200 and 600 MHz-km, for Multimode (MM) fibers and more than10GHz for single mode (SM) fibers), while for an electrical conductor, usually is between 10 to 25MHz-km,

ii.) Low attenuation of fiber optics enable longer cables runs and fewer repeater,

iii.) Optical fibers are unaffected from any electromagnetic radiation and do not emit any radiation,

iv) Optical fibers are easy to install, and their weight is 10-15 times lesser and the cost less than copper.

Optical fiber construction consist of core, cladding, buffer and jacket. A small core is the medium used to transmit light and has a core/cladding diameters of 8/125 μm. To realize total internal reflection, the refraction index of the cladding is less than the index of refraction of the core. The buffer (Ø = 250 μm) and jacket (Ø = 400μm) are to protect the core and cladding from any physical and environment damage. A schematic of an optical fiber is presented in Figure 2.2.

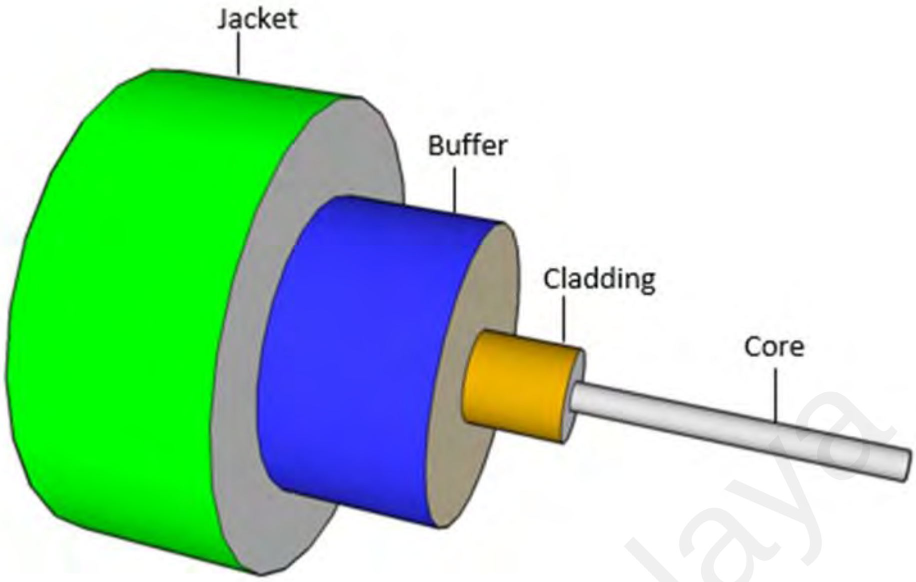

Figure 2. 2: Illustrative diagram of an optical fiber.

2.3 Laser Principles

Generation of laser radiation involves a few process that are absorption, spontaneous emission and stimulated emission. For the absorption, an electron at ground energy level (E_1) absorbed an incident photon and excited to higher energy level (E_2). When an electron at higher energy level (E_2), in general, the electron will eventually decay to the ground energy level (E_1), thus release a photon of radiation. This phenomenon is Spontaneous emission that emit photon in random direction and phase.

To generate laser, population inversion process is required. Population inversion occurs when the population at level 2 or density of excited two-level atomic system is more than population level 1 or density of the unexcited two-level atomic system ($N_2 > N_1$).

In this condition, the energy of E_{21}, will enable an electron at higher energy level (E_2) to decay toward ground energy level (E_1). The energy can be calculated by;

$$h\nu = E_{21} = E_2 - E_1 \qquad \text{(Eq. 2. 1,(Renk, 2012))}$$

The energy of E_{21} will be transferred in the form of electromagnetic wave which adds to the incident photon. This event is called as stimulated emission. This stimulated emission will exhibit emission that is identical to the incident photon (same wavelength, direction and phase). But if the condition is $N_2<N_1$, the active medium acts as an absorber. Figure 2.3 shows three mechanism:

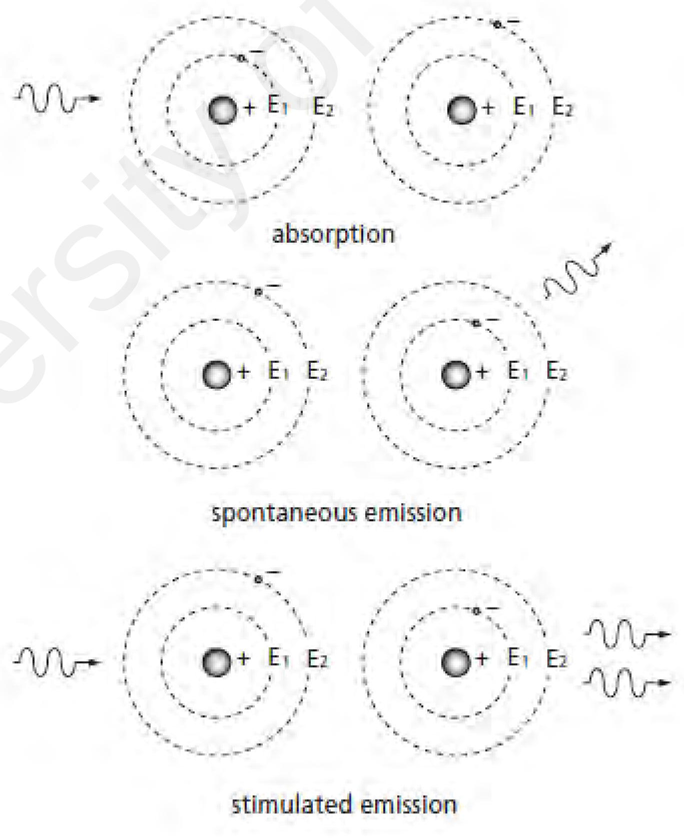

Figure 2. 3: The mechanism of absorption, spontaneous emission and stimulated emission(Svelto & Hanna, 1998).

The generation of laser by stimulated emission transition occur in gain medium. The spontaneous emission is generated by pumping the gain medium and the amplified to form amplified spontaneous emission (ASE). The basic laser setup presented in Figure 2.4. Its consists of excitation mechanism, laser resonator and lasing medium.

By continuously pumping the lasing medium, the population inversion will occur at lasing wavelength. When excited atoms start to decay, they exhibit photon in all direction spontaneously. Some photon travel along the lasing medium but mostly radiated out the sides. The photons travel along the axis of the lasing medium will stimulate the atoms when they tend to emit the photon. These photons will be reflected back into the lasing medium to stimulate more excited atoms.

When photons that travel out, they do not provide to the lasing process. When the photons reflected back and forth and contacting to more atoms, the spontaneous emission will eventually decrease and the stimulated emission on-axis predominates, then the laser will be generated.

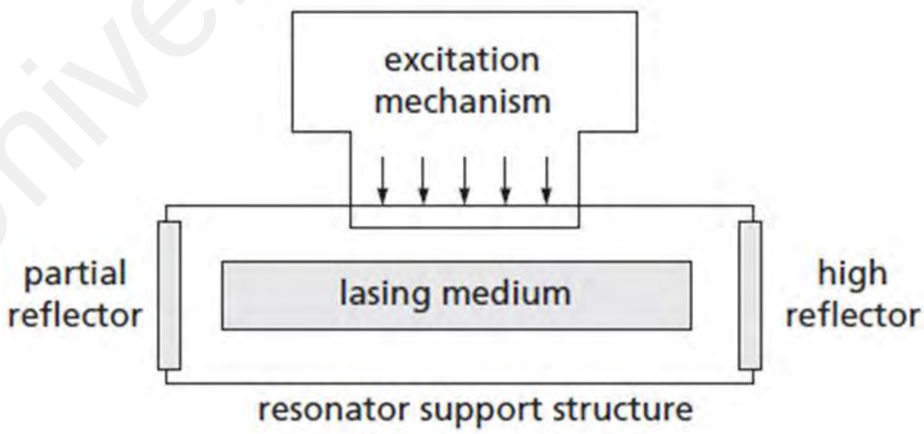

Figure 2. 4: Schematic diagram for basic laser.

2.4 Three and Four-Level Lasers

Figure 2.5 represent the schematic diagram of the three and four-level energy systems which represent the real process of generating laser. The three-level system involves three energy levels which are pump, upper lasing level (ULL) and lower-lasing level(LLL). For the three-level system, the energy is pumped through the gain medium to excite the atoms into above ULL. When the atoms start to decay to ULL because of heat emission and finally decay into the ground state. The transition from ULL to ground state produces the laser.

For the four-level system, there involves four level laser which are pump, upper lasing level, LLL and ground state. When the electron is pumped to higher than upper lasing level, it then decays to ULL and then to lower lasing level and then to the ground state. By continuous pumping process, a population inversion will happen and incident photon will be amplified coherently.

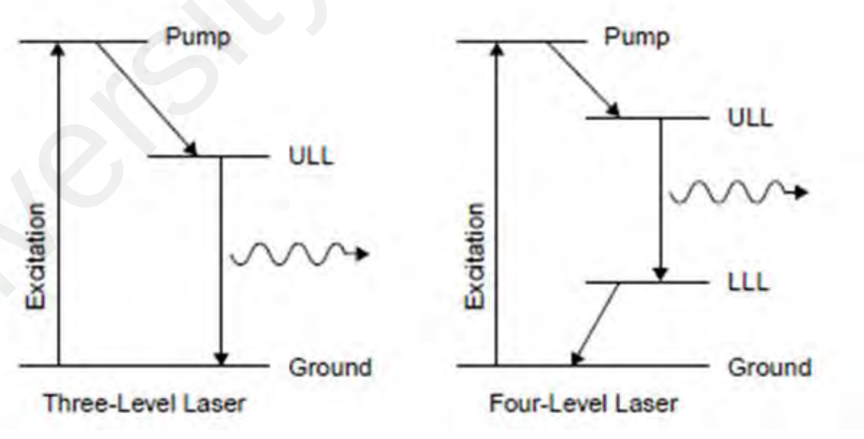

Figure 2. 5: A three and four-level laser pumping system(Csele, 2011).

2.5 Erbium-Doped Fiber (EDF) and Depressed Cladding Erbium-Doped Fiber (DC-EDF)

Conventional wavelength (C-band) is most important wavelength because of the lower loss in fiber optic communication which cover from 1530nm to 1560nm wavelength. Based on this reason, C-band has been selected as the wavelength of choice in optical communication. Several research have demonstrated a passive Q-switched laser obtained in C-band wavelength by employing an EDF as gain medium (B. Chen et al., 2015; Y. Chen et al., 2015; H. Guo et al., 2016; Li et al., 2015; Wu, Zhang, Wang, Li, & Chen, 2015).

However, to accommodate the future needs in optical communication, other wavelengths are currently being explored. A few research had been demonstrated on pulsed laser at S-band region by using DC-EDF as gain medium(Ahmad et al., 2017; Ahmad, Saat, & Harun, 2005; Ahmad et al., 2015).

2.5.1 Erbium-Doped Fiber (EDF)

Since the discovery of Erbium-Doped Fiber (EDF) in late 1980s, EDF has proven to be a material which is used in various applications such as broadband optical source, wide-band optical amplifier and tunable laser. The generation of Amplified Spontaneous Emission (ASE) in EDF produces high output power and broader optical bandwidth(Desurvire & Simpson, 1989). Since demonstration of Erbium-Doped Fiber Amplifier (EDFA) as optical amplifier, they attracted much interest in optical communication industry. In fiber laser application, the Erbium-Doped Fiber Laser (EDFL) is one of a most famous gain medium.

The core of an EDF gain medium is doped with rare earth element erbium ion (Er^{3+}). The EDF became a popular gain medium in fiber laser because their large gain bandwidth, typically ranging in tens of nanometer. The energy level diagram of Er^{3+} ions is represent in Figure 2.6. The laser 974nm is pump through the erbium-doped fiber and Er^{3+} ion is excited to level of E_3. After a while, the excited ions starts to decay to the E_2 through nonradioactive emission. Finally, the excited ions will falls to ground level through spontaneous emission and exhibit photon in 1520-1570nm wavelength region. The higher the pump power is pumped, the stronger the spontaneous emission amplified through entire fiber.

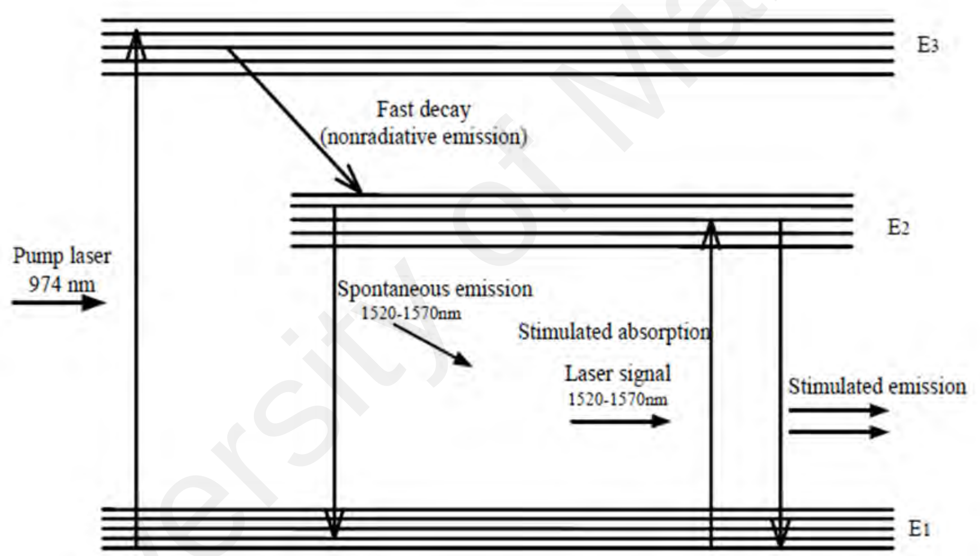

Figure 2. 6: Diagram of energy levels in Erbium-doped fiber (W. Zhu, Qian, & Helmy, 2015).

2.5.2 Depressed Cladding Erbium-Doped Fiber (DC-EDF)

DC-EDF is the solution of the shortcoming of EDF in S-band amplification. Generally, DC-EDF requires difference spooling diameter to obtain the laser within S-band amplification. The bending losses of the DC-EDF change accordance to bending diameter. The losses can reach high value when the bending too small. Furthermore, loss spectrum of tighter bends tends to shifts towards shorter wavelength which can be used to stop the formation of ASE in C-band wavelength region that give advantage to more shorter wavelength, S-band (Foroni, Poli, Cucinotta, & Selleri, 2006). These effect shown in Figure 2.7. The ASE spectra was measured using DC-EDF with various bending diameter (Foroni et al., 2006; Rosolem et al., 2005; Thyagarajan & Kakkar, 2004).

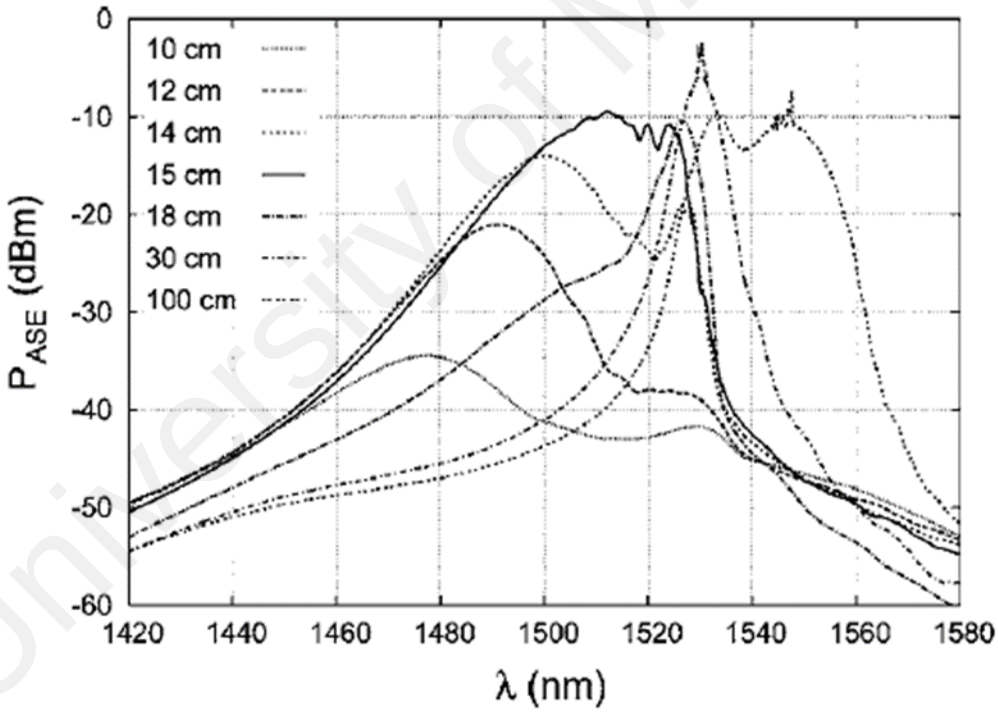

Figure 2. 7: ASE spectra measured using DC-EDF with various bending diameter. Reproduced from (Foroni et al., 2006)

Figure 2.8 represent the cross-sectional view of DC-EDF. At region I, there are consist of core radius r, range from $0 \leq r \leq r_o$. The depressed-cladding employ the region II, $0 \leq r \leq r_1$ with refractive index of n_1. Whereas region III lies at $r \geq r_1$ with refractive index of n_2.

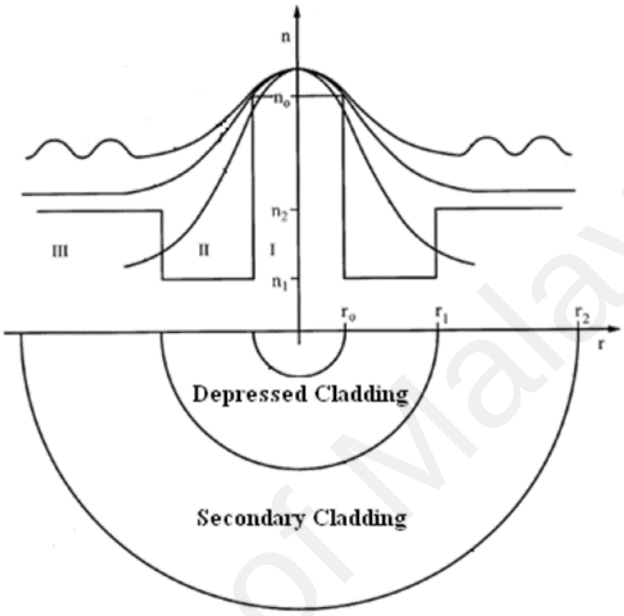

Figure 2. 8: DC-EDF cross-sectional view. Reproduced by (Arbore & Keaton, 2005)

2.6 Q-switching

In 1961, the Q-switched operation starts with Hellwarth, who has come out with an idea which a short pulses can be produce if optical resonator loss quickly changes form high to low value(Hellwarth, 1961). After a year, (Collins & Kisliuk, 1962) and (McClung & Hellwarth, 1962) proved their ideas with successful experimental demonstrations utilizing electrically switched Kerr cell shutter in ruby laser. Q-switched operation happens when the laser output of the cavity system is switched by controlling the resonator loss and thus, enables the generation of short pulses typically from nanosecond to picosecond.

Q-switch start to inhibit the feedback of light in gain medium when the gain medium is pumped continuously and will produces low Q in the optical resonator. This process generates the population inversion but since there is no feedback in the laser cavity, no laser is produced in this process. At the same time, stimulated emission continue to occur due to the gain medium being continuously pumped. After a certain time, the gain medium is saturated when the energy stored reaching their maximum value.

Suddenly, the Q-switch device switch rapidly from low to high Q which allows the feedback in the gain medium and starts to amplify the stimulated emission. Due to large energy stored in gain medium, the light intensity will build up very quickly and causes the gain depletion. As a result, a giant pulse produce from short pulse of light output which has high peak intensity. This process is called as Q-switching operation. The cavity Q-factor formula is as follow:

$$\mathbf{Q} = \frac{\mathbf{2\pi f_o}\varepsilon}{\mathbf{P}} \qquad \text{(Eq. 2.2(Hellwarth, 1961))}$$

Where f_o is resonant frequency, ε is energy stored in cavity $P = \frac{dE}{dt}$ is power dissipated.

Q-switched laser hold high potential and is widely used in applications which need a long duration of pulses such as environmental sensing and material processing are where Q-switched lasers are being utilized. Q-switching operations are divided into two types; active and passive.

2.6.1 Active Q-switching

Active Q-switching require an external modulators such as mechanical, electro-optical or acousto-optics(Koechner, 2006). This method offers more complexity due to high losses in cavity system from the external modulators itself. Because of this drawbacks, researcher begin to find new alternative which leads to discovery of the passive Q-switching operation that give compact geometry and more simpler setup(Svelto & Hanna, 1998).

2.6.2 Passive Q-switching

For passive Q-switching operation, the SA is employed into laser cavity system by replacing the external modulator. The cavity laser system consists of gain medium and a nonlinear absorbing medium. When the gain medium is pumped, the energy is developed in the gain medium and thus emit the photons.

The laser may build when the gain medium become saturates before the absorber but the laser cannot emit intense pulse, but if the photons flux develops up to the level that saturates the absorber first, the laser resonator will form a quick reduction occurs in intracavity loss cause the laser Q-switched will produce short and intense pulse(Welford, 2003).

From the Semiconductor Saturable Absorber Mirror (SESAM) model by Spühler and his group(Spühler et al., 1999), they presented important parameters in passive Q-switched which are, repetition rate, pulse energy and pulse duration. The equations are simplified in following Table 2.2.

Table 2. 1: Parameter of the Q-switched taken from SESAM model (Spühler et al., 1999).

Parameter	Model	Description	Eq.
Pulse duration	$\tau_p = \frac{3.52\, Tr}{\Delta R}$	Tr = cavity round-trips time ΔR= modulation depth	2.3
Pulse energy	$E_p = \frac{h\nu_l}{\sigma_l} A \Delta R \eta_{out}$	$h\nu_l$ = photon energy at lasing wavelength A= area mode σ_l = emission cross section of the laser material ΔR = modulation Depth η_{out} = output coupling efficiency	2.4
Repetition rate	$f_{rep} = \frac{go - (Ltot + \Delta R)}{2 \Delta R \tau_l}$	g_o = small signal gain coefficient per resonator round trip L_{tot} = total losses ($L_{tot} = T_{out} + L_p$); T_{out} is output coupler, L_p is parasitic losses. ΔR= Modulation depth τ_L=upper-state lifetime of the gain medium	2.5

Figure 2.9 shows the pulse cycle which involves four different phase which g(t), q_o, q(t), Δg, g and l are round-trip intensity gain coefficient, unbleached value of saturable absorber per round-trip (bleached value of the saturable absorber, q=0),loss coefficient of a saturable absorber, gain coefficient between the beginning and the end of the pulse (gain reduction; $\Delta g = g_i - g_f$), saturated intensity gain coefficient per resonator round-trip and total nonsaturable loss coefficient per resonator round-trip.

At phase 1, absorber is initially at an unbleached state. When the gained is pumped until unsaturated value of losses, a pulse can be produce, the equation as following:

$$g_i = l + q_o. \qquad \text{(Eq 2.6)}$$

Where q_o is unbleached value of saturable absorber per round-trip and Δg is gain coefficient between the beginning and the end of the pulse (gain reduction; $\Delta g = g_i - g_f$). The intracavity power, P start to rise slowly from spontaneous emission noise till enough intensity to cause the bleaching of saturable absorber.

Phase 2 begins when the SESAM is fully bleached (q=0) and when added this condition into Eq. 2.6, the new net gain which made the power grow rapidly until gain starts to deplete ,shown in Eq 2.7 :

$$g_i - 1 - q = q_o \qquad \text{(Eq. 2.7)}$$

The maximum pulse achieved when the net gain is zero. Further depletion occurs in phase 3 and the gain become negative which made the intracavity start to decays. However, in this phase, the pulse still coupled out powerful energy. At phase 4, when the pulse of the absorber recover, the gain needs to be pumped to the threshold level again before the next pulse can start(Spühler et al., 1999).

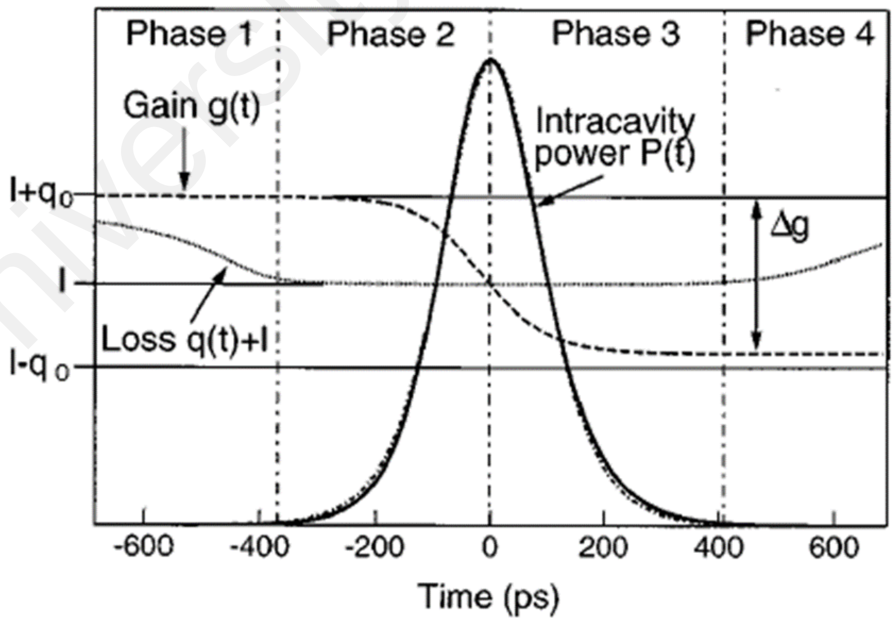

Figure 2. 9: The power, loss, and gain on time scale of the pulse width. After the gain surpass the loss, the power starts to develop. The peak of the Q-switched pulses is reached when the gain equals to the total losses (Spühler et al., 1999).

Another important parameters for SA are saturable absorption, nonsaturable absorption, the recovery time of the absorber, saturation intensity and absorption bandwidth which is influence by chemical the atomic structure of the SA. Saturable absorption, nonsaturable absorption and saturation intensity can be simply explained in a simple two-level nonlinear saturable absorption coefficient as indicated in Eq. 2.8. The saturable absorption is corresponding to the modulation depth and nonsaturable absorption that is expresses as a percentage of linear absorption(Bao et al., 2011).

$$\alpha(I) = \frac{\alpha_0}{1+\frac{I}{I_s}} + \alpha_{ns} \qquad \text{(Eq. 2.8)}$$

Where α_o is modulation depth, I is the incident light intensity, I_s is saturation intensity and α_{ns} is the nonsaturable absorption.

Figure 2.10 shows the nonlinear saturable absorption dynamic graph at different light intensity. When the light intensity produced less than the saturation intensity ($I < I_s$) in the laser resonator, lasing cannot occur and the optical absorption is high. When the laser is intensity more than or equal to saturation intensity ($I \geq I_s$), the absorption reduces and the transmissivity increases. The last condition is when the light intensity more than the saturation intensity ($I>>I_s$), the absorption is said to be saturated which cause a high Q-value in the resonator and starts the Q-switched laser oscillation.

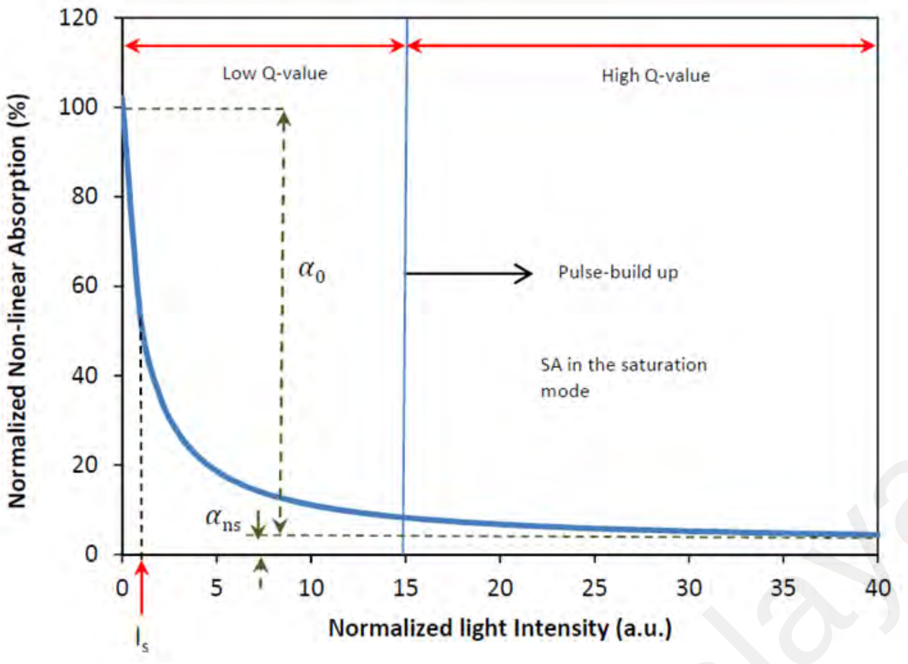

Figure 2. 10: The nonlinear saturable absorption dynamic against light intensity in Q-switching operation.

2.7 Principle of SA

The SA is a device which changes their absorbance in accordance to the power of the incident light. SA operation can be relate to the principle of nonlinear saturable absorption, the transmission is larger at low optical intensities at high optical intensity. Figure 2.11 shows the saturable absorption process in a two-level system. When high optical intensity pass through the SA, hv ≥ E_g (band gap energy of the SA), the saturable absorption will occurs and suddenly induced electron-hole pair as constructed in Figure 2.11 (a). Meanwhile, excess photon energy, (hv > Eg) will produce electron kinetic energy and release as heat. High optical intensity will result a bigger different in the absorption rates of the SA. This can be relate to Pauli Exclusion Principle, when excited state is fully occupied, the absorption net will reduce and make the material saturated. Afterwards, light cannot absorbed and leave the SA transparent for light transmission, as presented in Figure 2.11 (b). The excited-state absorption and electron-hole recombination will happen when the subsequent light enter the SA(Zulkifli, 2015).

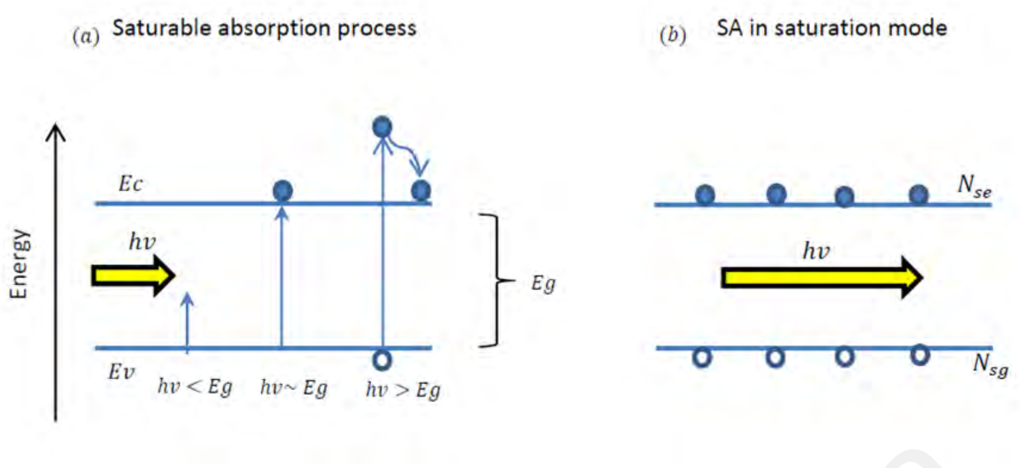

Figure 2. 11: Formation of electron-hole pair in the saturable absorber of two level system with (a) saturable absorption process and (b) saturated SA (Zulkifli, 2015).

Figure 2.12 shows the noise suppression of the saturaber absorber. When the saturaber absorber cooperated into the laser cavity system, the gain medium is pumped to produces the ASE. This ASE noise of a gain medium is shaped to be a pulse train and after a few round trips, the resulting high optical intensity that will oscillate the pulsed state(Kashiwagi & Yamashita, 2010).

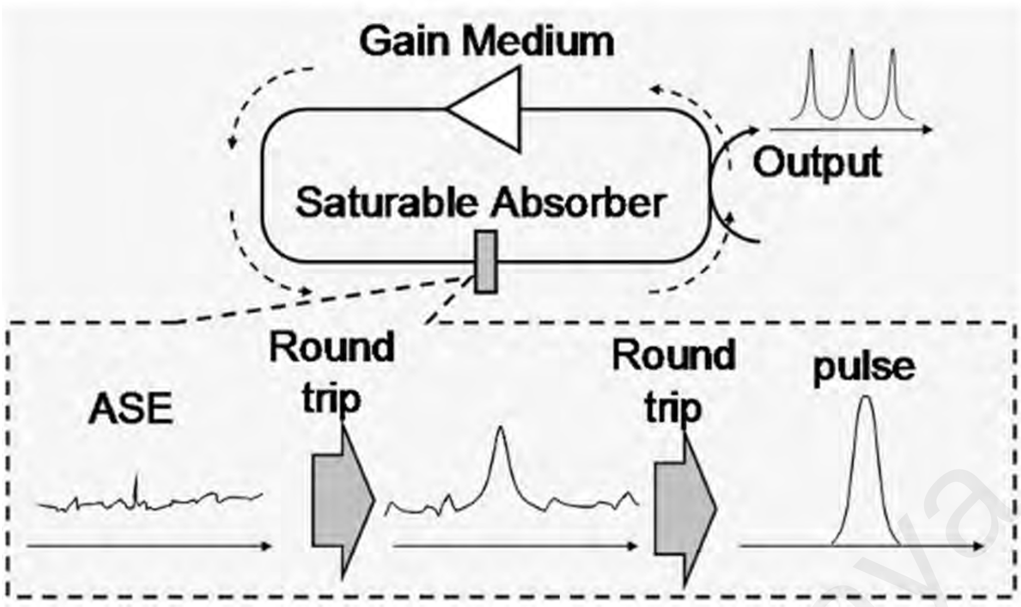

Figure 2. 12: Noise suppression of the saturable absorber (Kashiwagi & Yamashita, 2010).

Generally there have many method to generate passive Q-switched including Semiconductor Saturable Absorber Mirror (SESAM), transition metal-doped bulk crystal, graphene, carbon nanotube (CNT), transition metal di-chalcogenides (TMDs), topological insulator (TI) and black phosphorus (BP). However, SESAMs drawbacks from high fabrication cost, fragility, limited operation bandwidth and needs extra optical component including lens and mirrors which added more complexity and high loss in cavity design(Okhotnikov, Grudinin, & Pessa, 2004). Doped bulk crystals as SA also requires extra component such as mirror and lens to align the fiber output into the crystal(Laroche et al., 2002). The shortcomings of these two early approach has triggered researcher to find new SA which more compact and economical system.

2.8 Evolution of SAs

For years, silicon has been the base material for electronics, but now silicon is approaching its limit (Brunner & Moore, 1995; Schaller, 1997). Despite the effort to create multicore transistor, the maximum number of core that can benefit from this innovation is 16 (Franklin, 2015). Therefore, scientists are looking into nanomaterials as saviour. Research on 2D materials are blooming since the discovery of graphene (Novoselov et al., 2005). Graphene also has been using as saturable absorber to produce mode-locked (Bao et al., 2009; Sun et al., 2010) and Q-switched fiber lasers (J. Liu, Xu, & Wang, 2012; L. Q. Zhang, Zhuo, Wang, & Wang, 2011). After graphene, new categories of 2D materials emerge, such as TMDs and TI. These materials also haves been utilized as saturable absorbers for generating mode-locked and Q-switched lasers (Harith Ahmad et al., 2016; Kassani et al., 2015; Yan et al., 2017; H. Zhang et al., 2014; M. Zhang et al., 2015).

The remarkable discovery of graphene and carbon nanotube(CNT) are two carbon allotropes which used in widely application in optics and communication field due to their unique electronic and optical properties. Graphene, a two-dimensional crystalline carbon allotropes was discovered by Konstantin Novoselov and Andre Geim at University of Manchester(Geim & Novoselov, 2007). The graphene as ideal SA in passive Q-switched device are successfully demonstrated by many group which proven the graphene has ultrafast carrier dynamic(George et al., 2008) and large broadband optical absorption (2.3%/layer)(Kuzmenko, Van Heumen, Carbone, & Van Der Marel, 2008).

In addition, graphene absorb light at low intensity but transmit at very high intensity cause by their Pauli blocking property and has ultra-wideband operability due to linear dispersion of Dirac electrons. CNT has almost similar behavior as graphene which form atomic arrangement of carbon allotrope with cylindrical nanostructure was explored by Sumio lijima of NEC Corporation(Ajayan & Lijima, 1992). CNT also has a wideband operability even though not as wide as graphene because of the resonance energy dependence to the tube diameter. Discovery of graphene as SA provides question to researchers which is whether the other material that has the same type of Dirac material can produce saturable absorption.

TI is one of the Dirac material that produces Dirac-like linear band dispersion due to their band structure almost identical to the graphene structure(H. Zhang et al., 2009). Reported by François Bernad and Han Zhang, after they find out that the Tis has saturable absorption at telecommunication wavelength(B. Guo et al., 2015), they demonstrate passive mode-locking of Erbium-Doped Fiber laser using $BiTe_3$ nanosheets which is first demonstration photonic application of Tis. Besides that, $BiTe_3$ produces optical transmittance increase accordance to the saturable absorption of the material. $BiSe_3$ exhibit very high modulation depth which up to 95%(Zhao et al., 2012). However, TIs remarkable properties had opened a wide door to other 2D materials which may broadened the choice of the SA.

BP is another 2D material has band-gap depend on the layer of the material that changes from 0.35 eV(bulk) to 2 eV(monolayer)(Rudenko & Katsnelson, 2014). Reported by Yu Chen et al, they inserted the BP based SA device into all fiber laser cavity system resulting the generation of passive Q-switching with maximum pulse energy of 94.3nJ and passive mode-locking with maximum pulse width down to 946 fs(Y. Chen et al., 2015).

TMDs are also amongst the 2D materials, including molybdenum di-selenide ($MoSe_2$), molybdenum disulfide (MoS_2), tungsten di-sulfide (WS_2) and tungsten di-selenide (WSe_2)(Coleman et al., 2011; Reifler, Nuhfer, & Towe, 2014). Recently, many researchers using TMDs as SA for generation of Q-switched laser as reported a tunable range ytterbium-doped Q-switched fiber laser using a few layer of MoS_2 range from 1030nm to1070nm(Woodward et al., 2014).

Their group also demonstrated Q-switched laser based on $MoSe_2$ SA using ytterbium, erbium and thulium Doped fiber as gain medium. Besides that, experimental based on MoS_2 used in three different wavelength which are 1µm, 1.5µm and 2µ region to generate Q-switched laser successfully demonstrated as reported by Zuo et al(Z. Luo et al., 2014). Furthermore, Chen et al reported that they used four different SA which are TMDs(MoS_2, $MoSe_2$, WS_2 and WSe_2) to generated Q-switched laser resulting the highest modulation depth is $MoSe_2$ and WS_2 gain the most stable pulses compared to the others(B. Chen et al., 2015). In conclusion, TMDs material as saturable absorber are promising material used in photonics and optoelectronic application.

Because of too saturated information and experiment of the material mention above, metal nanomaterials such as SNPs has attracted great interest among the researchers. Furthermore less research on this SNPs as SA, so its good opportunity to explore this performances of this material as SA in fiber laser application.

2.9 SNPs

Nanoscience and nanotechnology field has gained rapid development over the last twenty years. The advancement in this field mostly depend on the capability to synthesize the nanoparticles from many types of materials, sizes, shapes and the efficiently to gather them into more complex architectures. Nano-sized material garnered significant interest from many researchers due to their unique electronic and optical properties that different from their bulk state (Alivisatos, 1996). Size-dependent of these material already been proved experimentally in numerous electronic and optical device (Ellingson et al., 2005). At the same time they in studied to understand and can control the collective properties of the nanoparticles (Lu, Liu, & Lee, 2005; Markovich et al., 1999; Reinhard, Siu, Agarwal, Alivisatos, & Liphardt, 2005)

Metal nanoparticles including SNPs hold substantial roles and widely used in optoelectronic (Rustad, 2001), photonics(Maier et al., 2001), surface-enhanced Raman scattering(Maier et al., 2001; Nie & Emory, 1997), information storage(Murray, Sun, Doyle, & Betley, 2001), biological labelling (Nicewarner-Pena et al., 2001) and formulation of magnetic Ferro fluids (Pileni, 2001). The first exploration of optical properties of metal nanoparticles colloidal suspensions and ultrathin metal film is by Michael Faraday in 1850s(Faraday, 1857). Then follow by Gustav Mie that published experimental works on extinction of light by metal sphere which leads to his significant achievement in 1908(Mie, 1976). Generally, the optical characteristics metal nanoparticles rely on its plasmon surface which means the collective oscillations of the free electrons in the metal nanoparticles itself. The plasmon resonant peaks and line width are very sensitive to size(Van Dijk et al., 2006), shape of the nanoparticles(El-Sayed, 2001; Jin et al., 2001; Kelly, Coronado, Zhao, & Schatz, 2003), the species of the metal(Mulvaney, 1996) and the surrounding medium(Mulvaney, 1996) .

2.9.1 Properties of Silver Nanoparticles (SNPs)

SNP is one of transition metal which technologically important materials that have found many in many applications. Transition metals are d-block element are placed from group-3 to group-12 in periodic table that also known as metallic in nature as shown in Figure 2.13. The valence shell electrons of silver metal placed in the d-orbital and are loosely bound and which contribute to high electrical conductivity.

21 Sc 44.9559 Scandium	22 Ti 47.867 Titanium	23 V 50.9415 Vanadium	24 Cr 51.9961 Chromium	25 Mn 54.938 Manganese	26 Fe 55.845 Iron	27 Co 58.9332 Cobalt	28 Ni 58.6934 Nickel	29 Cu 63.546 Copper	30 Zn 65.4089 Zinc
39 Y 88.9058 Yttrium	40 Zr 91.224 Zirconium	41 Nb 92.9064 Niobium	42 Mo 85.94 Molybdenum	43 Tc 98 Technetium	44 Ru 101.07 Ruthenium	45 Rh 102.9055 Rbodium	46 Pd 106.42 Palladium	47 Ag 107.8682 Silver	48 Cd 112.411 Cadmium
71 Lu 174.967 Lutetium	72 Hf 178.49 Hafnium	73 Ta 180.9497 Tantalum	74 W 183.84 Tungsten	75 Re 186.207 Rhenium	76 Os 190.23 Osmium	77 Ir 192.217 Iridium	78 Pt 195.084 Platinum	79 Au 196.9666 Gold	80 Hg 200.59 Mercury

Figure 2. 13: The element of the transition metal in the periodic table.

SNP gained scientific and practical attention since before 1980s due to their highly dispersed support to improve signal from organic molecules in Raman Spectroscopy application(Creighton et al., 1979; Lee & Meisel, 1982). In 1980s and 1990s, SNPs become highly potential material in advancement new-generation electronic, optical and sensor devices due to extraordinary combination of unique properties of optical properties with the surface plasmon resonance (SPR), well-developed surfaces, catalytic activity, double layer capacitance and etc(Henglein, 1989). Over the last few decades, the rapid development of modernization of technology triggered the number of scientific publication that dedicated to synthesis and analyzation properties of the SNPs. SNPs has very excellent and unique optical properties and ability to amplify signals from fluorescence and Raman Spectroscopy (Jin et al., 2003; Taton, Mirkin, & Letsinger, 2000; J. Zhang, Malicka, Gryczynski, & Lakowicz, 2005)

2.9.2 SNPs based SA

The potential of the SNPs as being a saturaber absorber substantiated after successful experimental implementation of SNPs in field of photonic devices (F. Chen et al., 2014; Glubokov et al., 2014; Qi et al., 2014; V. Singh & Aghamkar, 2014). Based on the past research by (Glubokov et al., 2014) resulting the Ag-doped bismuthate glasses has a large and ultrafast third-order optical nonlinearities and the absorption band of Ag-doped sample can be longer than 1400nm. Besides that, SNPs is associated with $Er^{3+/}Yb^{3+}$ co-doped telluride glasses to enhance the fluorescence intensity at 1.53µm(Qi et al., 2014). All these improvement has enhanced the generation of local electric field effect due to localized Surface Plasmon Resonance (SPR) of SNPs(Qi et al., 2014). In addition, the SNPs induces the highest electrical and thermal conductivities amongst all the metal(Gasaymeh, Radiman, Heng, Saion, & Saeed, 2010). Furthermore, passively mode-locked successfully generate by using plane polygonal SNPs as saturable absorber(Glubokov et al., 2014). Hence, these nonlinear optical properties with saturable loss of SNPs can hold high potential as SA(Kim, Husakou, & Herrmann, 2010).

Very recently, H. Guo and his group presented the SNPs as SAs by using depositing method at the end of the facet. From their experiment, SNPs shows large modulation depth and stable Q-switched at C-band wavelength region(H. Guo et al., 2016). Reported by (Ahmad, Samion, Muhamad, Sharbirin, & Ismail, 2016), they generate passively Q-switched by using thulium-doped fiber as gain medium. Pulsed obtained highly stables which no fluctuations over one hours. Table 2.2 presented the comparison of performance of various type of SAs.

Table 2. 2: Comparison of performance of various type of SAs. Taken from (H Ahmad, NE Ruslan, MA Ismail, et al., 2016).

SA	Modulation Depth(%)	Saturation Intensity ($MWcm^{-2}$)	Repetition rate(kHz)	Pulse width(µs)	Maximum pulse energy (nJ)	Ref
Ag	18.5	_	17.9 - 58.5	11.4 – 2.4	132	(H. Guo et al., 2016)
MoS_2	9.3	15.9	7.0 x 10^3	8.0 x 10^{-6}	N/A	(H Zhang et al., 2014)
$BiTe_3$	95.3	480	1.2 x 10^3	1.21 x 10^{-6}	N/A	(H. Zhang et al., 2009)
$MoSe_2$	4.7	3.4	26.5 - 35.4	18.9 – 9.2	825	(Woodward et al., 2015)
BP	18.6	10.74	7.0 – 15.8	39.8 -10.3	94.3	(Y. Chen et al., 2015)

CHAPTER 3: FABRICATION AND CHARACTERIZATION OF SILVER-NANOPARTICLES FILM

3.1 Introduction

Over past few years, SNPs has gained high traction in sensor applications due to their extraordinary optical, electronic and chemical properties (Schultz, Smith, Mock, & Schultz, 2000; Taton et al., 2000; Yguerabide & Yguerabide, 1998). There a various ways used to prepare metal oxide nanoparticles(Pal, Shah, & Devi, 2007; Rosemary & Pradeep, 2003). Among them are reverse micelles process(Kumar & Rani, 2013; Maillard, Giorgio, & Pileni, 2002; Xie, Ye, & Liu, 2006), salt reduction(Pillai & Kamat, 2004), microwave dielectric heating reduction(Patel, Kapoor, Dave, & Mukherjee, 2005), ultrasonic irradiation(Salkar, Jeevanandam, Aruna, Koltypin, & Gedanken, 1999), radiolysis(Soroushian, Lampre, Belloni, & Mostafavi, 2005), solvothermal synthesis(Starowicz, Stypuła, & Banaś, 2006) and electrochemical synthesis(S. Liu, Huang, Chen, Avivi, & Gedanken, 2001; J.-J. Zhu, Liao, Zhao, & Chen, 2001). Very recently, demonstrated the generation of passive Q-switched using SNPs as SA. They fabricated three types of (according to nanoparticle size) using solvothermal method. They successfully demonstrated the saturable absorption properties is rely on the average size of the SNPs. The average size of sample 1, 2 and 3 are 70nm, 76nm and 94nm, respectively(H. Guo et al., 2016).

In this section, material characterization and nonlinear properties such as modulation depth and saturable absorption of the SNPs as SA are calculated. Nonlinear optical properties of semiconductors are broadly used in in application science and technology such as Q-switching(Fan et al., 2005), mock locking(J.-L. He et al., 2004), up conversion lasing(G. S. He, Markowicz, Lin, & Prasad, 2002) and optical limiting(Maciel, Rakov, de Araujo, Lipovskii, & Tagantsev, 2001).

In this research, raman spectroscopy, absorption spectrum and modulation depth using balanced twin detector method were investigated to confirm the existence of SNP in thin film, to determine the absorption spectrum of the SNP SA and to measure the modulation depth of the SNP SA, respectively.

3.2 Preparation and characterization of thin film SNPs as a SA.

SNPs powder was attained from Sigma Aldrich Malaysia and is used without further purification. The nanostructures sizes of the SNPs estimation of average sizes are in the range of 20-50nm. The fabrication of the silver nanoparticles thin film began by embedding 1.0 gram of SNPs powder into methyltrimethoxylane (MTMS) to transform the SNPs powder into thin film. 5.0 ml of MTMS and 5.0 ml ethanol were mixed together at weigh ratio of 1:1 with SNPs powder (5%) to form SNP SA thin film. The mixture was then ultrasonificated for 15 minutes. Afterwards, 0.5 ml sulfuric acid was added into the mixture and ultrasonicated again for 5 minutes. Finally, the mixture is poured into a petri dish and dried in room temperature for 3 days. The thickness of the thin film measured to be 0.15 ± 0.01 mm. Figure 3.1(a) shows a piece of SNPs thin film and (b) the microscopic image of the SNPs thin film.

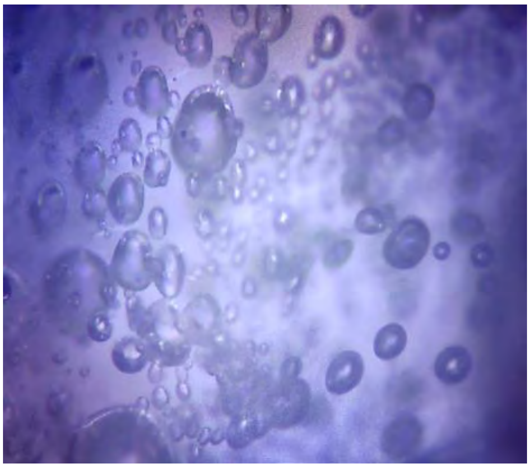

(a) (b)

Figure 3. 1: (a) a peace of the SNPs thin film and (b) Microscope image thin film.

3.2.1 Raman spectroscopy

Raman spectroscopy measurement of the silver-nanoparticles film is carried out using laser excitation at 532nm (green laser) with 10% laser power for 20 seconds. Figure 3.2 shows the Raman spectra patterns for silver-nanoparticles film with and without silver nanoparticles. The spectroscopy is performed using green light laser (532nm) with only 10% power of 50 mW. As seen in the figure 3.2(a), there are two well-defined prominent peaks of MTMS monomer and MTMS-based cubic crystals are observed at 248, 2912 and 2979 cm^{-1} which can be appointed to C-H stretching vibrations from methoxy and methyl groups in silane monomer. The results almost similar to reported works by (Jung, Kim, Hah, & Koo, 2009). Figure 3.2(b) constructed the raman spectrum after SNPs are added into the host material MTMS. Strong band in the range of 1300cm^{-1} to 1700 cm^{-1} that two well-defined prominent peaks at 1385 cm^{-1} and 1588 cm^{-1} are corresponding to Ag-O stretching and deformation vibration, respectively. The results obtained attributed to SNPs and similar with reported works by (Yukna, 2007) and the peaks same as figure 3.2(a) which belong to MTMS host material. Therefore, it is confirmed the SNPs are exist in the thin film.

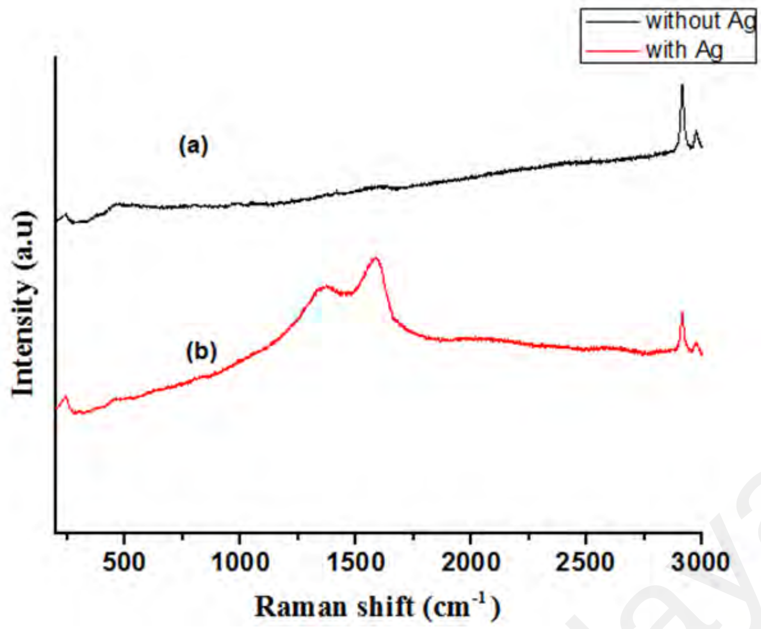

Figure 3. 2: Raman spectra of silver nanoparticles at 5mW (a) without silver nanoparticles and (b)with silver nanoparticles.

3.3 Modulation depth measurement of SNPs SA.

The saturable absorption spectrum was measured as shown in figure 3.3 (a). The absorption of the SA is 7 dB and the modulation depth of the SNPs thin film was characterized using balanced twin-detector method. High peak power reduces the absorption of light by the material. The saturable absorption of the material expressed as,

$$\alpha(I) = \frac{\alpha_s}{1+\frac{I}{I_s}} + \alpha_{ns} \qquad \text{(Eq. 3.1,(Garmire, 2000))}$$

Where $\alpha(I)$, α_s, α_{ns}, I and Is are intensity dependent absorption coefficient, saturable losses and non-saturable losses, laser intensity and saturation intensity, respectively. The modulation depth, which is defined as the difference of the maximum to the minimum light intensity holds substantial optical parameter that is describes the strength of optical field and SA material. Saturation intensity is defined as the optical intensity needed at steady state to reduce the 50% of the absorption from its unbleached value.

Figure 3.3 (b) represent the experimental set up of saturable absorption of silver-nanoparticles film employing a homemade mode-locked fiber laser with a measured pulse width, 0.53ps and a repetition rate of 27.7MHz and central wavelength, λ_c of 1560nm. After the optical amplifier with pulse duration increases from 0.53ps to 0.96ps. Then the optical amplifier is coupled to an optical attenuator and connected to 50/50 output couple. As seen in the inset of Figure 3.3(c), the modulation depth and saturation intensity calculated to be 31.6% and 0.54 MWcm^2.

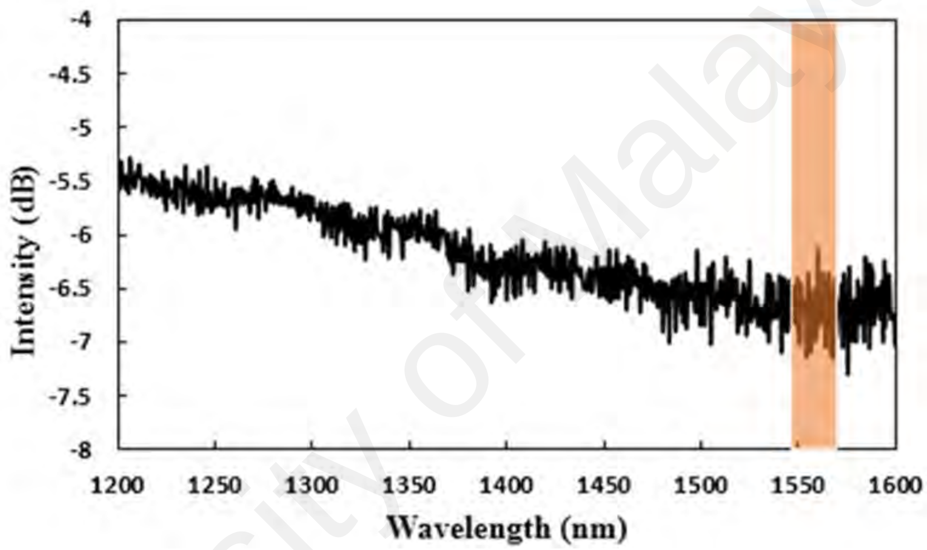

(a)

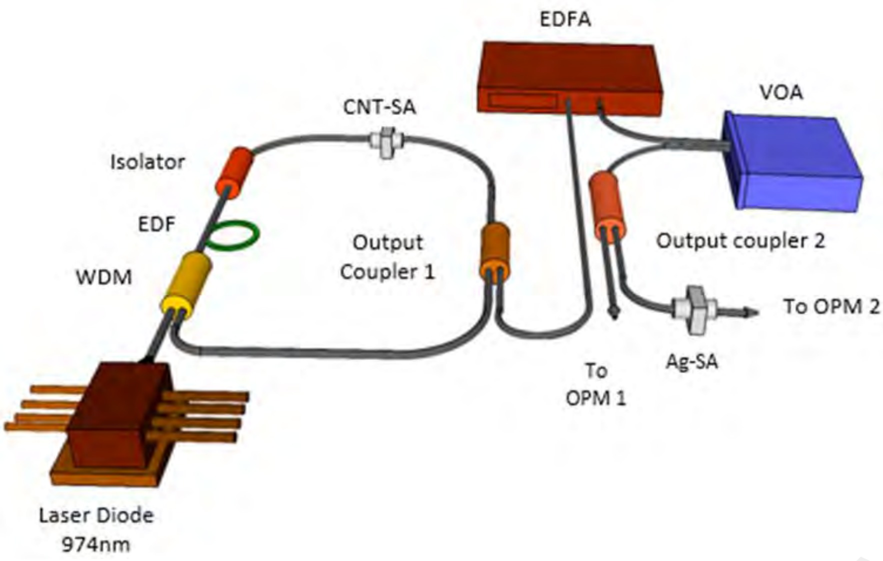

(b)

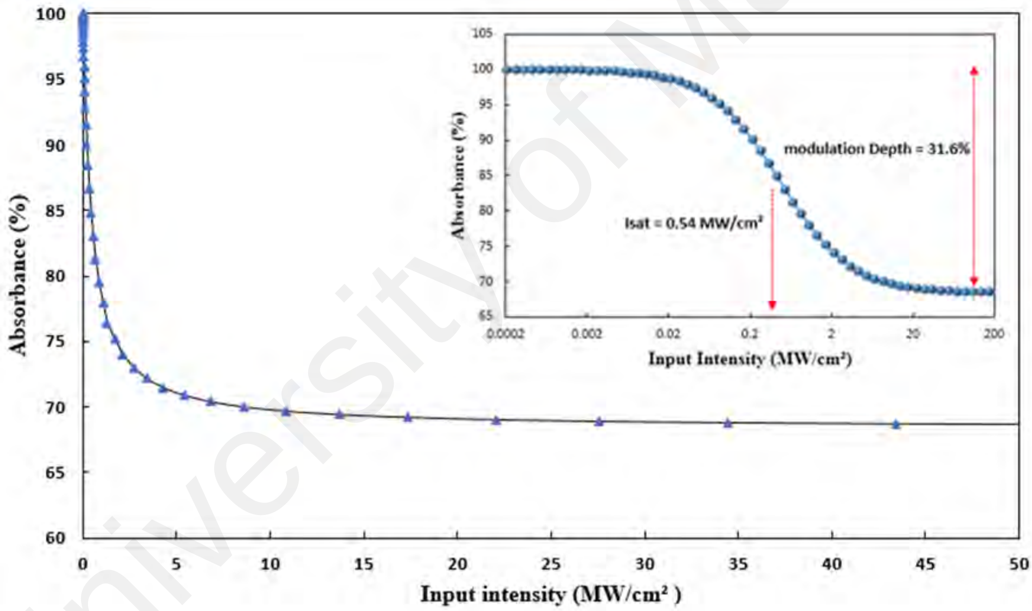

(c)

Figure 3. 3: (a) The saturable absorption of SNPs thin film (b) The experimental set up of the saturable absorption measurement and (c) measured saturable absorption of SNPs-SA.

CHAPTER 4: GENERATION OF PASSIVELY Q-SWITCHED USING SILVER-NANOPARTICLES AS SATURABLE ABSORBER IN C- AND S- BANDS REGION WAVELENGTH

4.1 Introduction

Q-switching operation plays an important role in laser systems to generate short and high intensity pulses. There are two types of Q-switched laser: active and passive. Active Q-switching required complicated devices such as electro- or acousto-optic modulators. Passive Q-switching can be achieved using several methods using saturable absorber or artificial saturable absorber. Semiconductor saturable absorber mirrors (SESAMs)(Keller et al., 1996) and single-walled carbon nanotubes (SWCNT)(Dong, Hu, Liaw, Hao, & Yu, 2011) are widely used as saturable absorber, whereas artificial saturable absorber can be achieved using nonlinear polarization rotation (NPR) method (Nelson, Jones, Tamura, Haus, & Ippen, 1997). Of all these techniques, SA is the most preferred method due to their compact size, easy to incorporate into laser cavity and relatively cheaper than active modulator. Numerous research are reported on metal nanoparticles such as silver and gold nanoparticles due to their remarkable optical properties such as large third-order nonlinearity, broadband surface plasmon resonance(SPR) absorption and fast response time (Cheng et al., 2010; Qin-Yong, Yong, Ji-Chuan, & Da-Yong, 2011) which highly potential to be used in optics, medicine and spectroscopy(Iga, Seki, & Watanabe, 2004; Moskovits & Suh, 1984; M. Singh, Singh, Prasad, & Gambhir, 2008). In this work will explore SNPs as SA in formed of thin film to produce passive Q-switched laser.

The used of various potential SAs with combination of EDF to generate passive Q-switched fiber laser in C-band region holds high potential in many application such as telecommunication, spectroscopy, range finding and material processing(Gräf, Staupendahl, Krämer, & Müller, 2015; Nissilae & Kostamovaara, 1993).

There also gained huge interest amongst researches to explore passive Q-switched laser at shorter wavelength which is in S-band region exploiting DC-EDF as gain medium.

In this chapter, the experimental set up at different wavelength, which is C- and S- bands laser cavity with employment of SNPs as saturable absorber are described. This chapter also discusses the generation of passively Q-switched by using EDF and DC-EDF as gain medium in ring configuration to generate laser at C- and S- bands wavelength to measure substantial parameters such as repetition rate, pulse width, pulse energy, peak power and output power.

4.2 Passively Q-switched by using silver-nanoparticles thin film as a saturable absorber at C-band wavelength.

4.2.1 Experimental Set up

Figure 4.1 showed the ring cavity configuration for generation of passive Q-switched fiber laser by employing silver nanoparticles thin film as SA. The ring cavity laser is pumped by 974 nm laser diode (LD) with 260 mW maximum pump power through a 980/1550nm wavelength division multiplexer (WDM). A 3-m long erbium doped fiber is used as gain medium. The silver nanoparticles thin film SA which is sandwiched between fiber ferrule incorporated into ring cavity acts as passive Q-switcher. An isolator was inserted into the ring cavity to ensure the unidirectional light propagation. Next, the output from the laser cavity is extracted by a 90:10 optical coupler, further splits by a 50:50 optical coupler so that we can take two measurement simultaneously. An Yokogawa AQ6370C optical spectrum analyser(OSA) and Yokogawa DLM2054 oscilloscope were used simultaneously to measure for optical spectrum and pulse train. During experiment, outputs powers were also measured by swapping one of the measuring device to optical power meter (OPM).

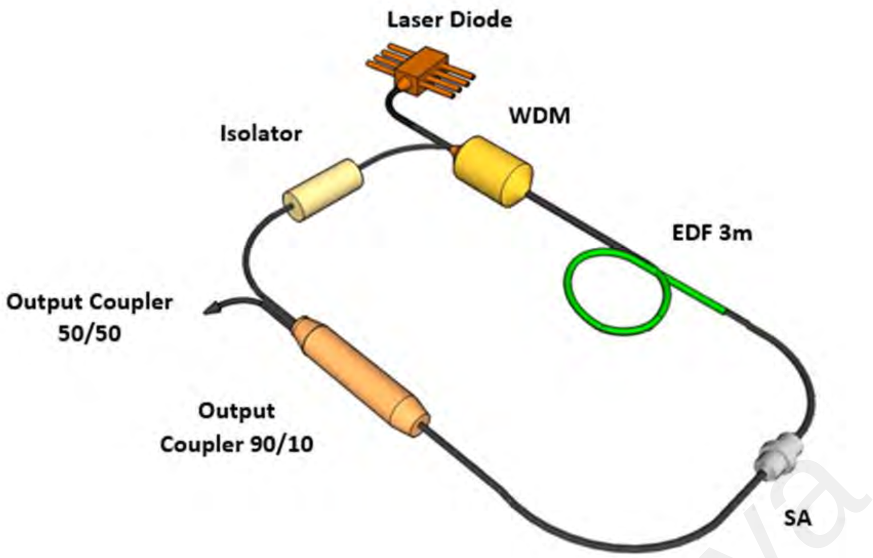

Figure 4. 1: The schematic diagram for generation of passively Q-switched fiber laser by employing silver-nanoparticles as a saturable absorber. Where WDM = wavelength division multiplexer, EDF= Erbium Doped Fiber, SA= saturable absorber.

4.2.2 Performances of Q-switching operation at C-band region

The performance of the passive Q-switched using SNPs based is observed. The operation of continuous wave laser started at pump power of 8.7 mW and self-starting Q-switched is achieved after pump power is increased to 20 mW. Stable Q-switched pulses is attained by further increase the pump power from 20 mW to 260 mW. Beyond this range, there no Q-switched detected. Figure 4.2 indicates the example of the pulse train at 50 mW , 90 mW,80 mW and 150 mW. The repetition rate increase as pump power increase exhibits a common characteristic of Q-switched pulses. The reliance of pulse repetition rate and pulse duration against the pump power is due to the nonlinear dynamic in the gain medium. When the pump power increased, more gain provided to saturate the SA material. Energy stored in the gain medium will emit a pulse and resulting the rapid generation of pulse which reducing the pulse width and increment the repetition rate(Degnan, 1995; Svelto & Hanna, 1998).

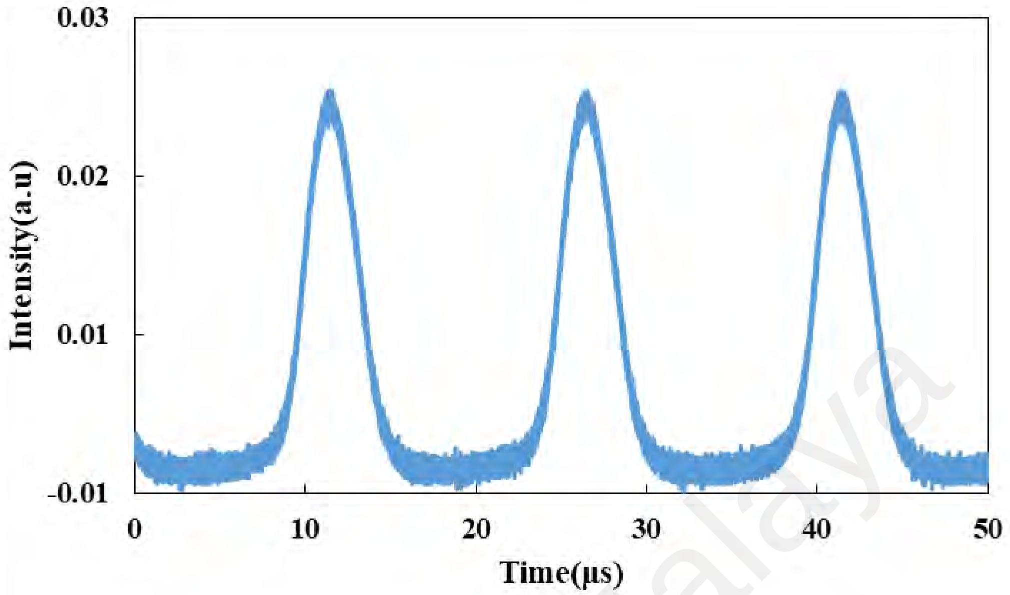
0.03
0.02
0.01
-0.01
Intensity(a.u)
0
10
20
30
40
50
Time(μs)

(a)

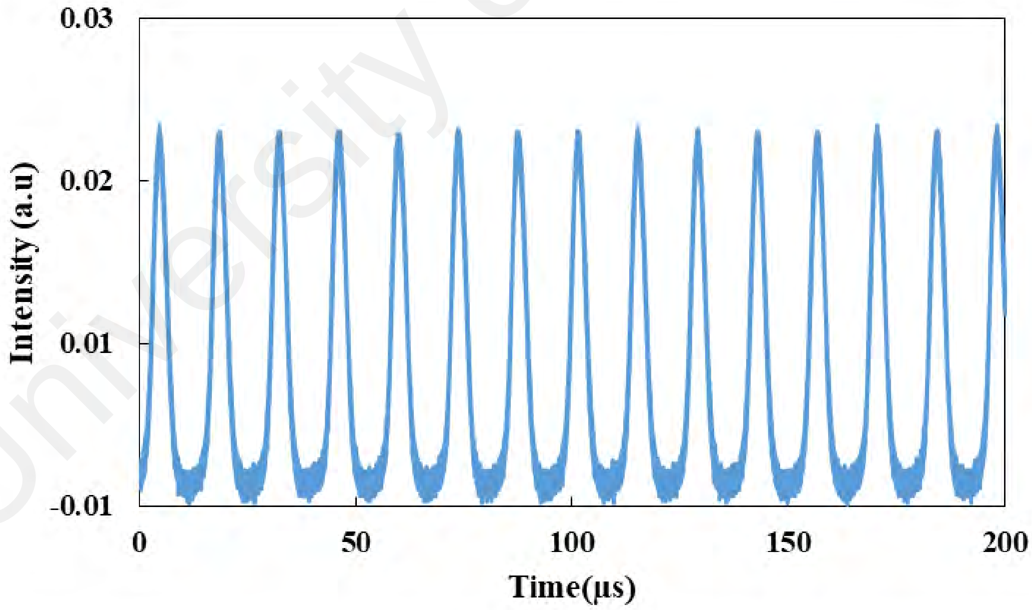
0.03
0.02
0.01
-0.01
Intensity (a.u)
0
50
100
150
200
Time(μs)

(b)

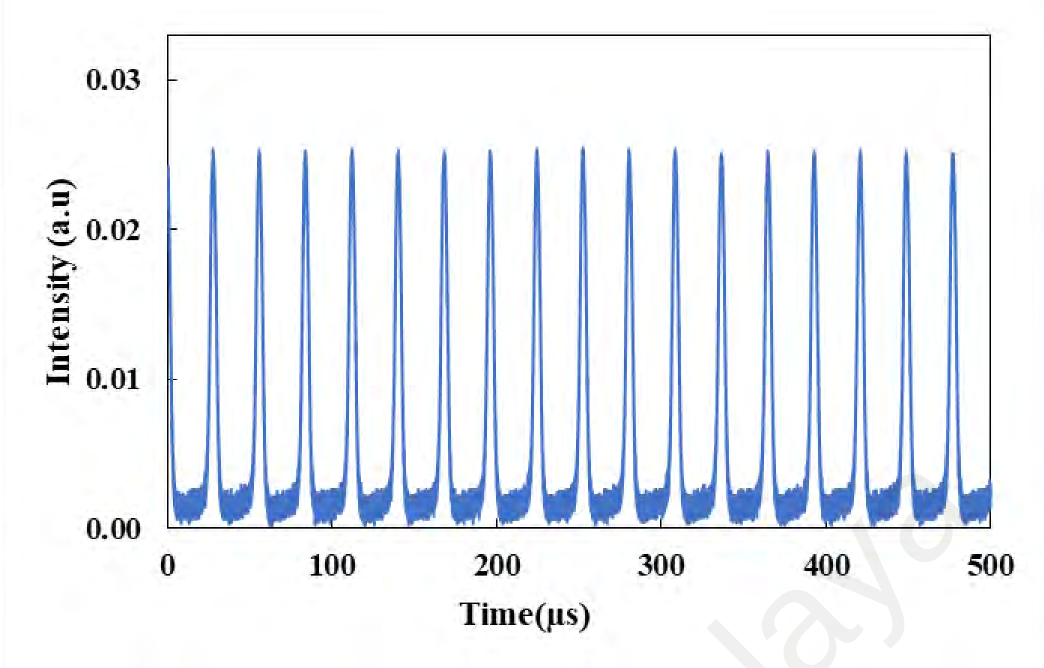

(c)

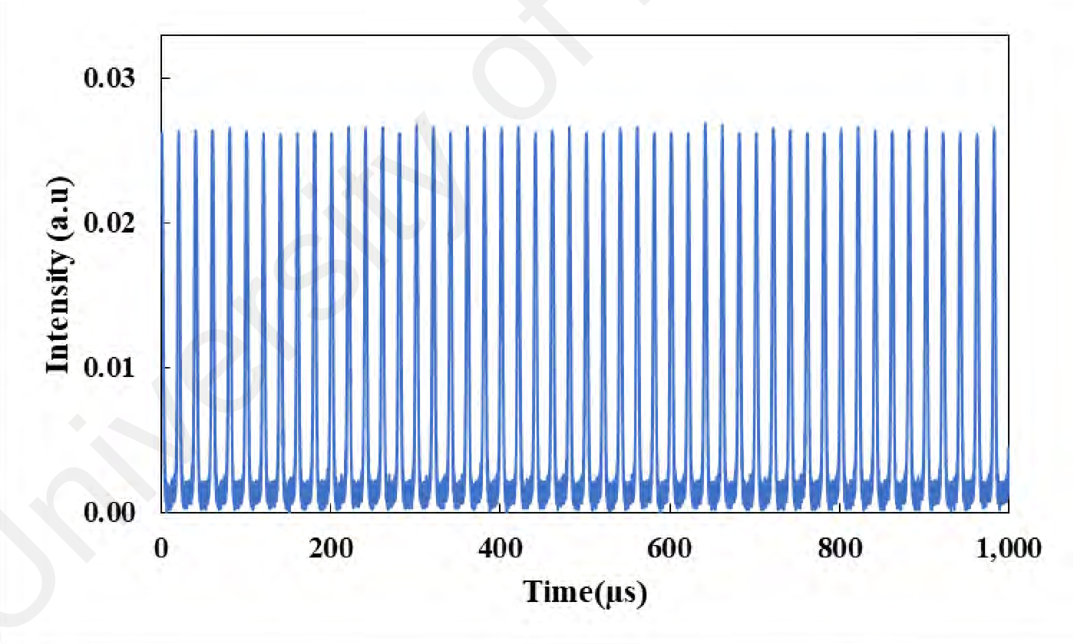

(d)

Figure 4. 2: Q-switched pulses train at different pump powers (a) Pp= 50 mW, f= 31.8 kHz, (b) Pp = 90 mW, f=37.7 kHz (c) Pp = 80 mW,f=34.5 kHz and (d) Pp = 150 mW, f=48.8 kHz.

Figure 4.3 represent the central wavelength of optical spectrum is 1558.7nm which located in C-band region. The spectrum broadening as the result of nonlinear phenomenon of self-phase modulation (SPM). The SPM is a nonlinear optical effect which occurs at the highest intensity of light. The distance between the pulses is 25.52 micron. The single pulse profile at this pump power has full width at half maximum(FWHM) of 4.02 micron. RF Spectrum with 300Hz resolution indicates the Q-switch has signal-to-noise ratio (SNR) which is measure of the signal to the level background noise give the value of 35dB which indicates good stability of the pulse train(Popa et al., 2011).

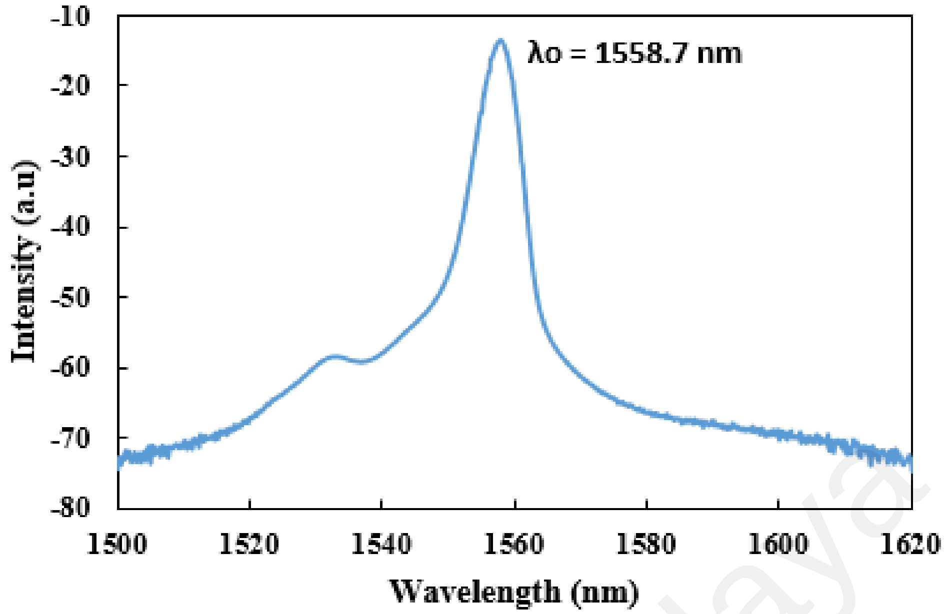

λo = 1558.7 nm
Intensity (a.u)
-10
-20
-30
-40
-50
-60
-70
-80
1500
1520
1540
1560
1580
1600
1620
Wavelength (nm)

(a)

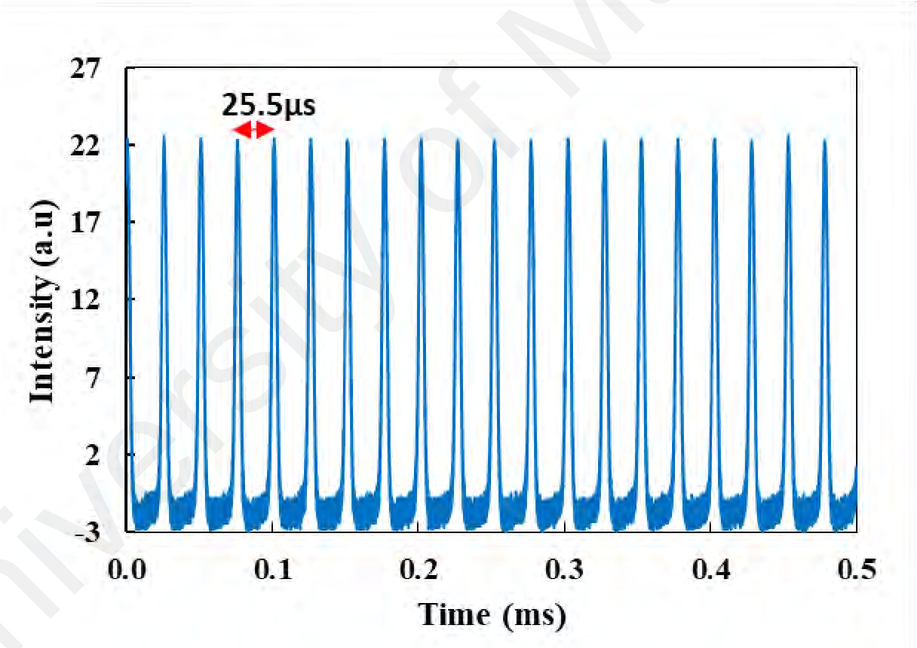

25.5μs
Intensity (a.u)
27
22
17
12
7
2
-3
0.0
0.1
0.2
0.3
0.4
0.5
Time (ms)

(b)

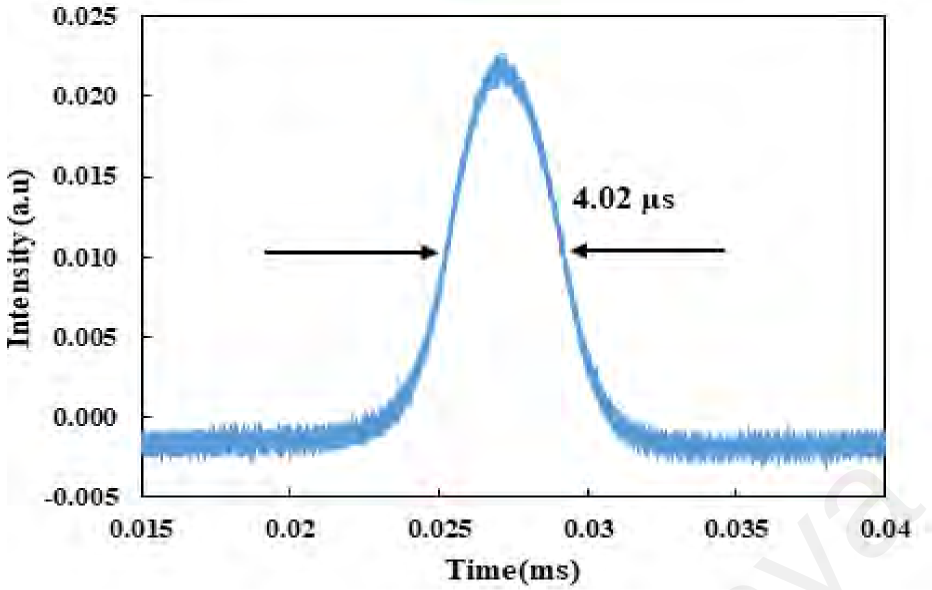

(c)

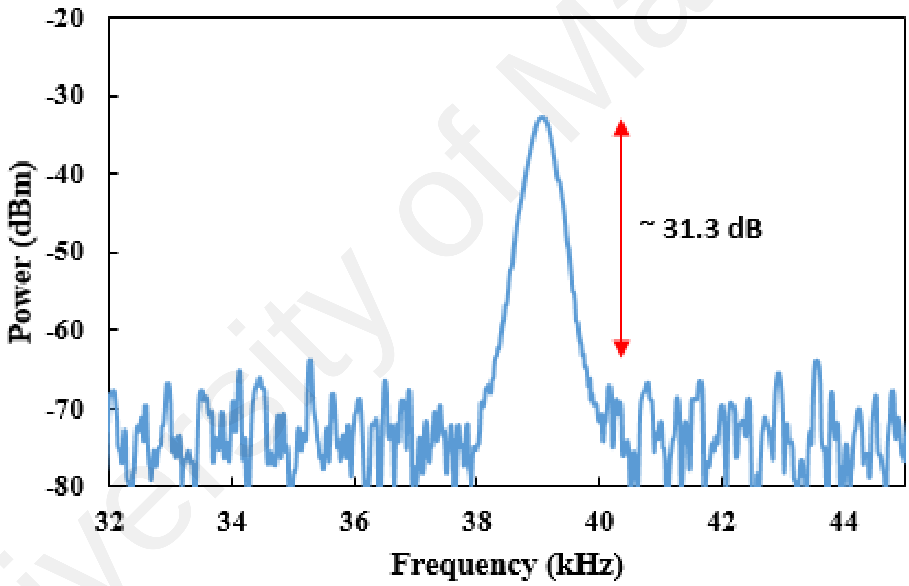

(d)

Figure 4. 3: The laser performance at 100 mW power pump. (a) Optical spectrum with central wavelength of 1558.7nm (b) Oscilloscope trace with pulse duration of 25.5μs. (c) Single-pulse profile (d) RF spectrum at frequency of 39.2 kHz.

Figure 4.4(a) shows pulse duration and repetition rate against pump power. When the pump power is increased from 20 – 260 mW, the repetition rate also increase in linear fashion from 19.4 kHz to 74.1 kHz while the pulse duration become shortening from 8.88 – 3.2μs. This phenomenon shows common characteristic of the Q-switching operation, as the pump power increase, more power circulates in the cavity system thus saturates the SA faster. The pulse duration had approached its limit as shown in Figure 4.4(a), which is related to modulation depth, SA become almost saturates because the smaller changes of pulse duration. Pulse properties relies on the nonlinear absorption in the gain medium. This results dependence on the pulse repetition and pulse duration on the pump power. A pulse will emit when the SA is saturated. Thus greater pump power will provide more gain which enables the laser operates in higher repetition rate with short pulses.

For Figure 4.4 (c), the graph peak power and pulse energy and become almost flat at beyond 170mW because the formula of the pulse energy is output power over the repetition rate and for the peak power, the pulse energy over the pulse duration. So the result trends will be influence by the graph (a) and (b) as well. Based on the measurement display in Figure 4.4(a) as well as (b) the peak power and pulse energy can be calculated. The maximum peak power and pulse energy are 2.55 mW and 8.17 nJ.

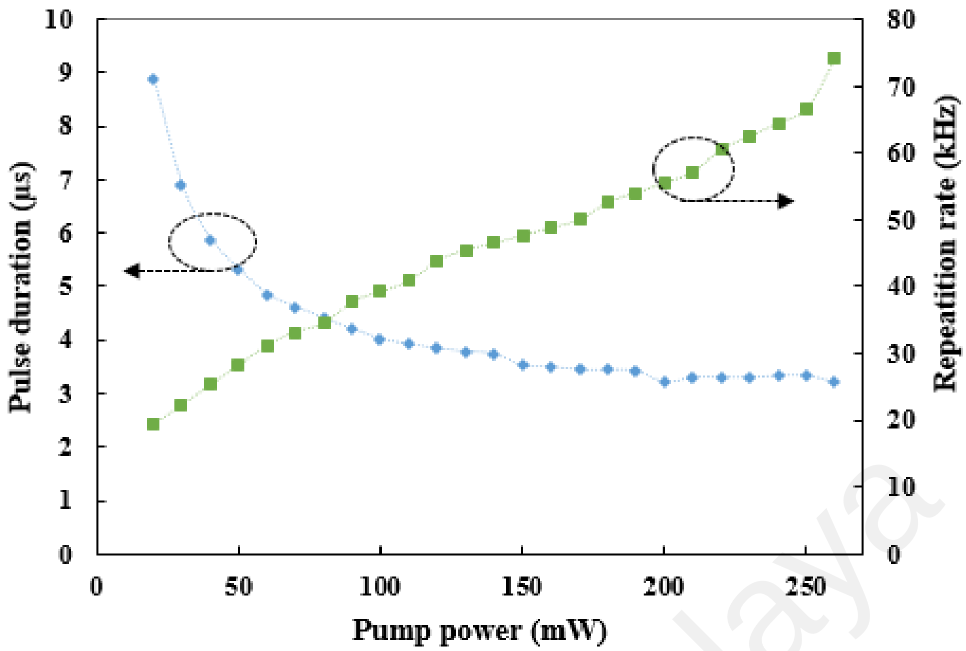
Pulse duration (µs)
Repeatition rate (kHz)
Pump power (mW)
0
1
2
3
4
5
6
7
8
9
10
0
10
20
30
40
50
60
70
80
0
50
100
150
200
250

(a)

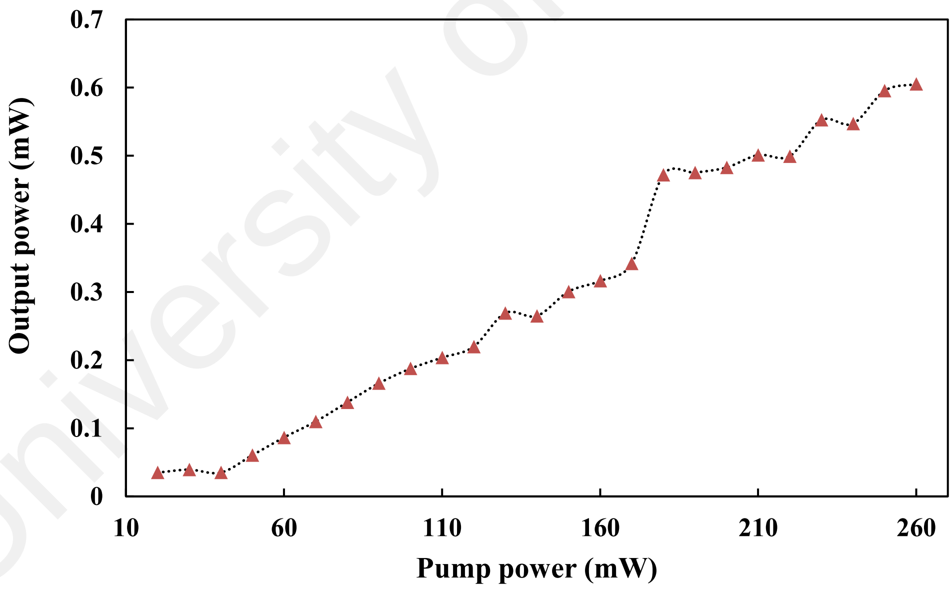
Output power (mW)
Pump power (mW)
0
0.1
0.2
0.3
0.4
0.5
0.6
0.7
10
60
110
160
210
260

(b)

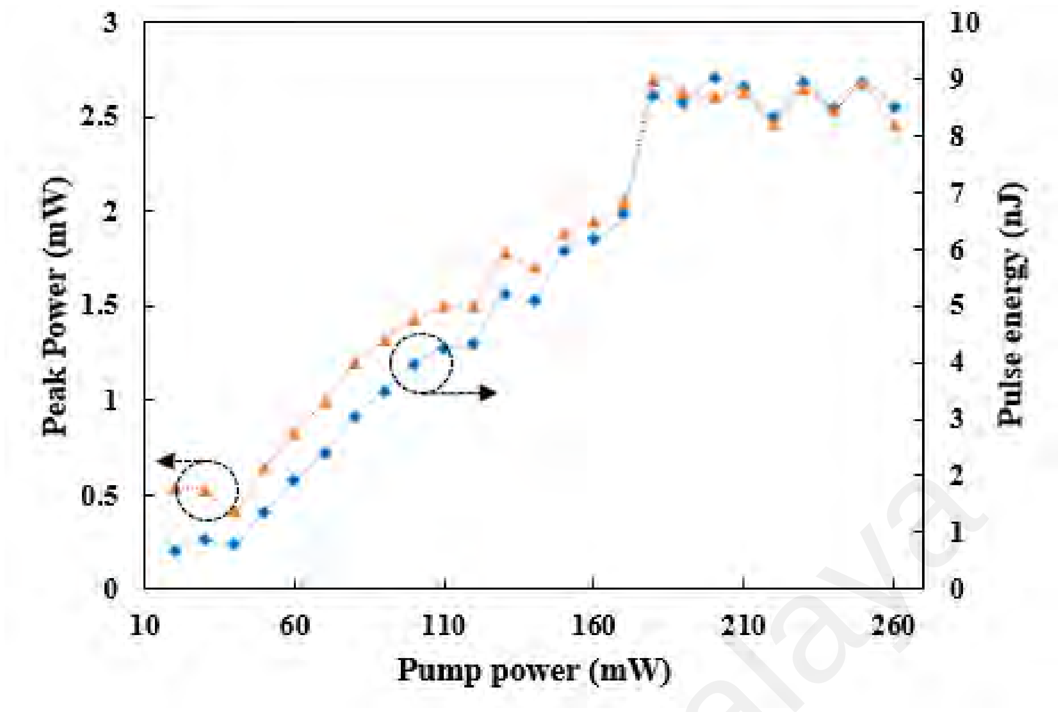

(c)

Figure 4. 4: The measurement of (a) Pulse repetition rate and pulse duration against pump power. (b) Output power against pump power and (c) Peak power and pulse energy against pump power

4.2.3 Tuning range Characteristic of Q-switched at C-band region wavelength based SNPs based SA.

Even though passive Q-switched fiber laser at single-wavelength widely used in various application, the formation of tunable Q-switched fiber laser also gained interest amongst the researcher for area such as spectroscopy(Y. Chen et al., 2014) and communication(Han et al., 2014). A few groups of researcher demonstrated the tunability experiment using Fiber Bragg gratings (FBGs)(Ahmad, Zulkifli, Muhammad, Zulkifli, & Harun, 2013; Dong, Hao, Liaw, Lin, & Tjin, 2010; Zhou, Wei, Dong, & Liu, 2010), Mach Zehnder interferometer(A.-P. Luo, Luo, & Xu, 2009) and tunable filter(Antonio-Lopez, Castillo-Guzman, May-Arrioja, Selvas-Aguilar, & LiKamWa, 2010). Tunable filter is wavelength selective mechanism for simple tunable of q-switched fiber laser(H Ahmad, NE Ruslan, ZA Ali, et al., 2016).

This experiment demonstrated a passively Q-switched fiber laser with broadband wavelength tunability using erbium-doped fiber laser (EDFL) with SNPs –based SA and TBPF. To observe the performances of the Q-switching operation, initially the tunable bandpass filter is fixed at 1558.4 nm wavelength which the lowest cavity losses. The Q-switched operation occurred at 20mW. Stable Q-switched pulses is detected up until 160mW. Tunability of Q-switched fiber laser is performed by tuning the tunable filter. As shown in Figure 4.5, the tunability of SNPs film varied from 1552.9 to 1580.2nm which covered 27.3nm at partially S- and C- bands region wavelength.

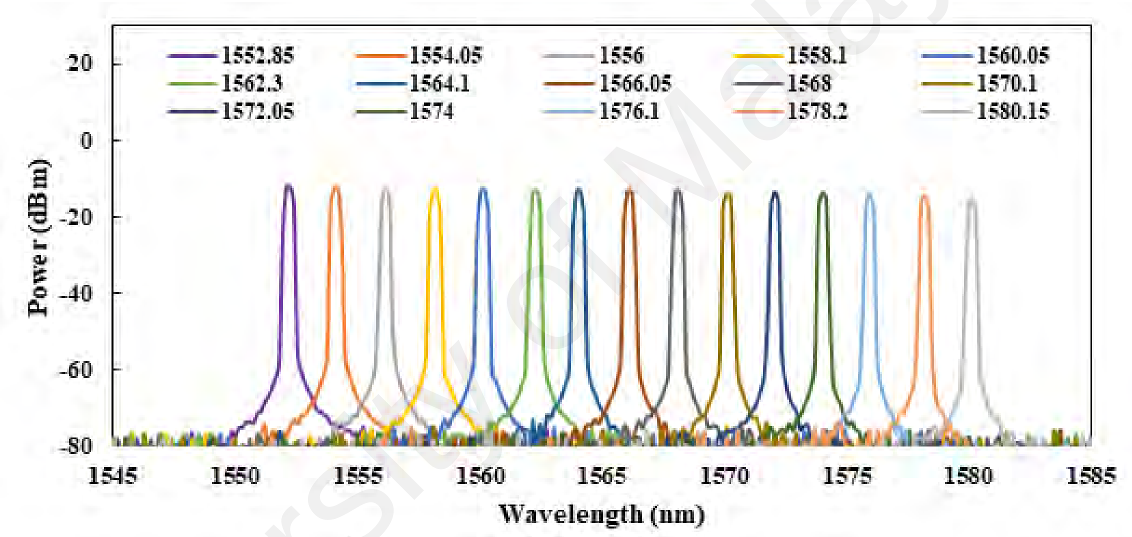

Figure 4. 5: Optical Spectra at different wavelengths.

Figure 4.6 represents the repetition rate against output wavelength which proved the dependence of the repetition rate on wavelength. Figure 4.6 shows the stable Q-switched pulse trains recorded by the oscilloscope at different wavelengths at fixed pump power,30 mW (a) 1556.0nm (f=21.8kHz), (b) 1554.1nm (27.7kHz), (c) 1558.1nm(20.4kHz) and (d) 1562.3nm(19.2kHz) .

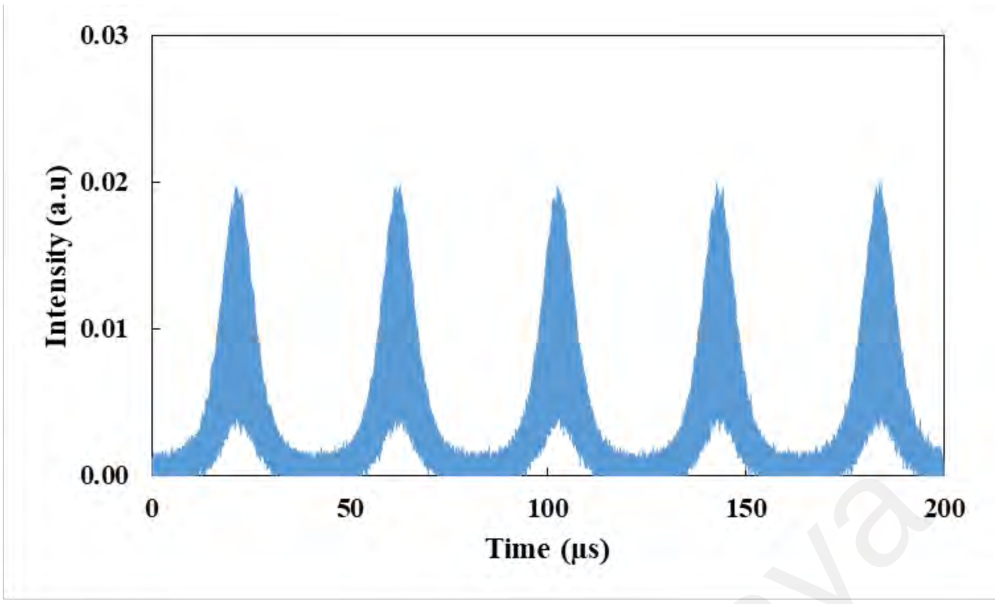
0.03
0.02
0.01
0.00
Intensity (a.u)
0
50
100
150
200
Time (µs)

(a)

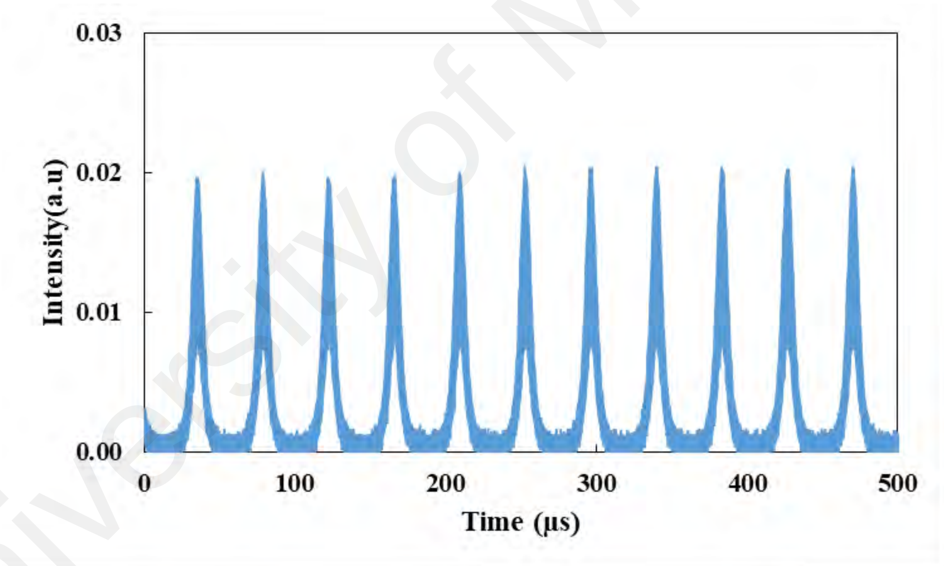
0.03
0.02
0.01
0.00
Intensity(a.u)
0
100
200
300
400
500
Time (µs)

(b)

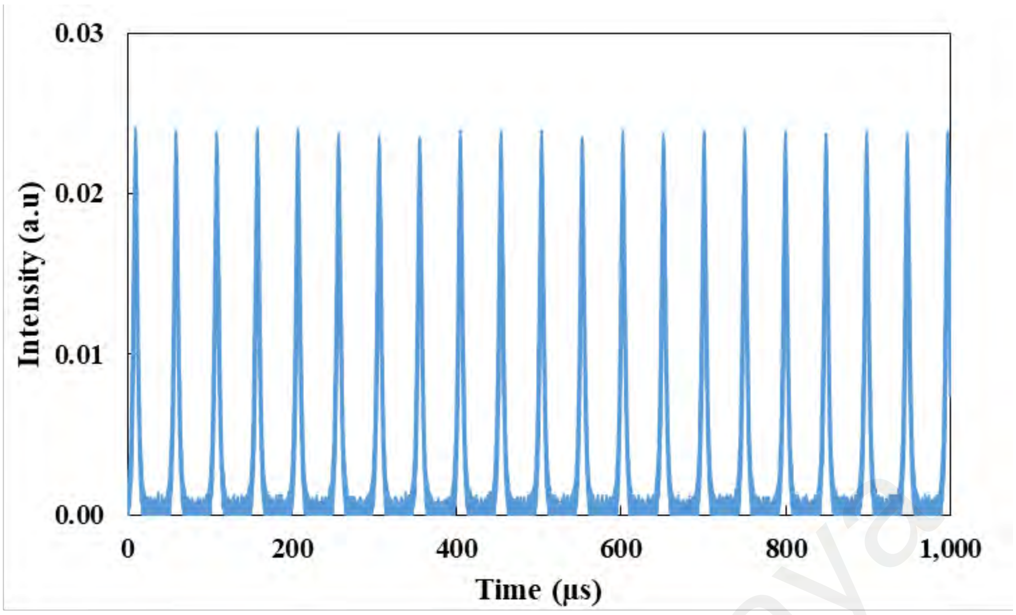

(c)

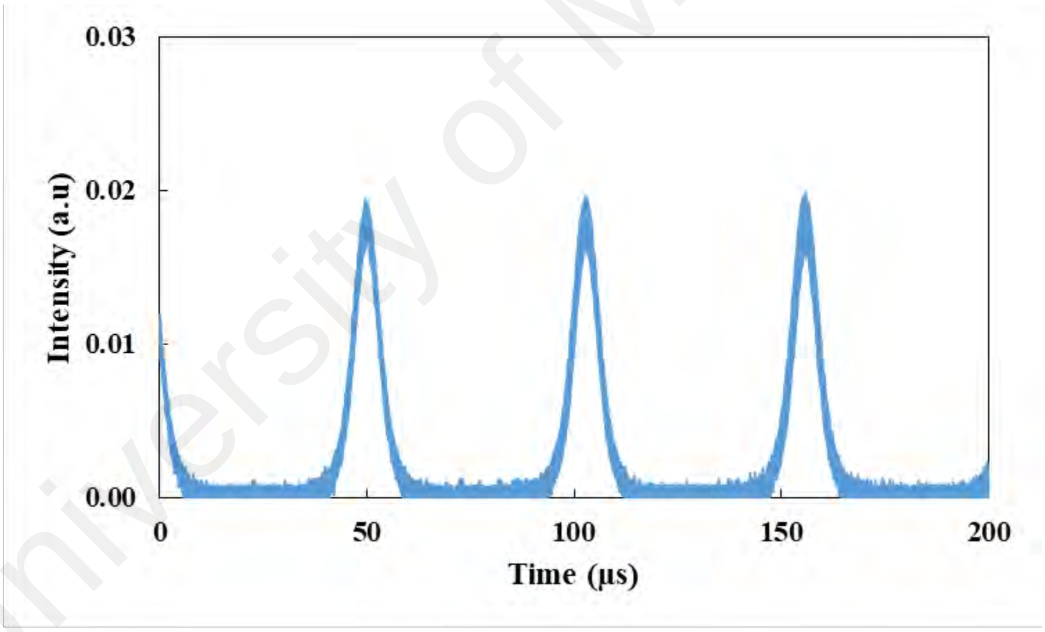

(d)

Figure 4. 6: Pulse trains of Q-switching operation at wavelength (a) 1556.0nm,(b)1554.1nm,(c)1558.1nm and (d)1562.3nm at fixed pump power.

The relationship of repetition rate, pulse duration and the output power against different wavelength are shown in figure 4.7. At fixed power 30mW, the wavelength is tuned from 1552.9nm to 1580.2nm resulting in decreasing of repetition rate from 24.4 kHz to 10.5 kHz. As highlighted in figure 4.7(a) ,the trend of repetition rate obtained similar to the trend of ASE spectrum because its attributed by the variation of the ASE gain which the larger gain gives a larger repetition rate and larger average output power(Zhou, Wei, & Liu, 2012). The output power decreases from 0.07 mW to 0.04 mW as plotted in figure 4.7(b).

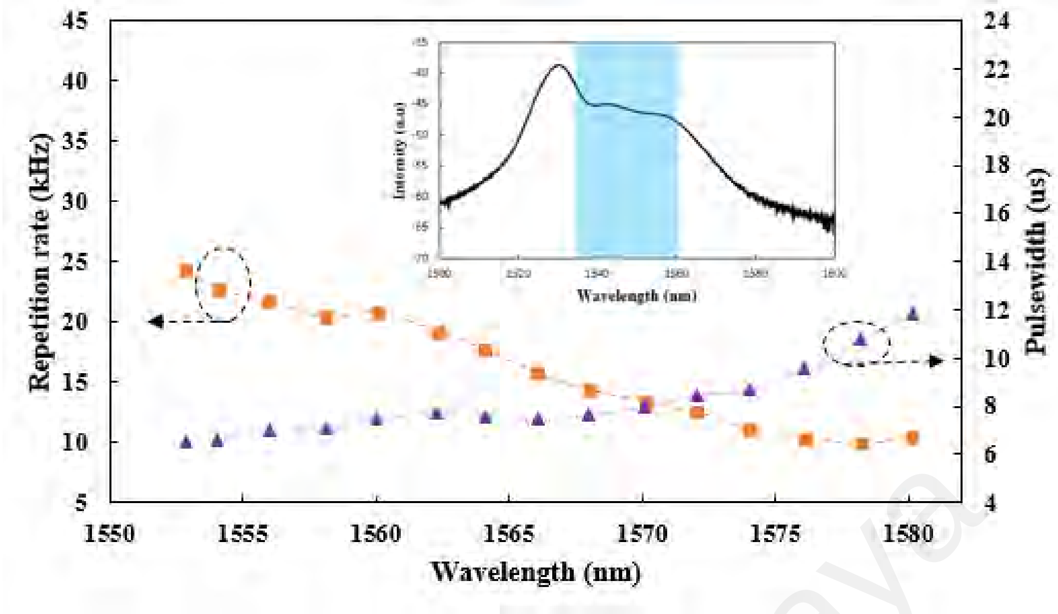

(a)

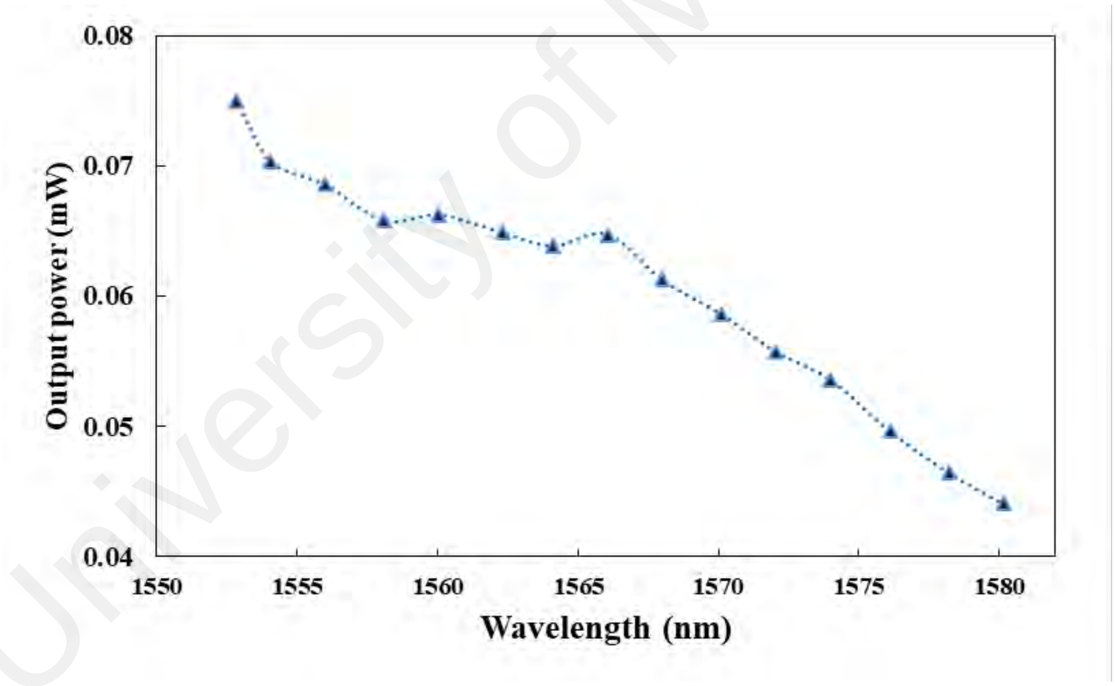

(b)

Figure 4. 7: Pulse repetition rate and pulse duration against the pump power and (b)Output power against wavelength.

4.3 Passively Q-switched DC-EDF by using SNPs based SA at S-band wavelength.

4.3.1 Experimental Set up

Figure 4.8 shows ring cavity fiber laser to generate passively Q-switched using silver nanoparticles saturable. The gain medium used in this work is a DC-EDF with absorption coefficient of 7.6 dB/m (974 nm), the core composition is made of 2.5% GeO2, 5.5% Al2O3 , 92% SiO2 and 0.15 wt.% Erbium, and the depressed cladding composition is made of 3% fluorine, 0.5% P2O5 and 96.5% SiO2. A 974 nm LD, with maximum pump power of 400 mW, is used to excite the DC-EDF through a WDM. The common port of the WDM is coupled to the DC-EDF. A polarization insensitive isolator is put inside the cavity system to provide a unidirectional light propagation in cavity system. A 95/5 optical coupler was used to extract out 5% of the total energy for measurement purposes. The extracted energy is then coupled to a 50/50 optical coupler to measure the repetition rate with pulse width and output power at same time.

In-order to characterize our laser pulse, we used an Yokogawa AQ6370C OSA ,an Yokogawa DLM2054 oscilloscope, a Anritsu MS2683A radio frequency spectrum analyser (RFSA) with an DET01CFC ultrafast photodetector and an OPM. The SA is sandwiched between two fiber ferrules and employ into the laser cavity after the 95% port of the optical coupler. All optical components used in the experiment are polarization independent. The lasing threshold is 30 mW. Without a saturable absorber, the CW operation continued until the pump power was set to maximum.

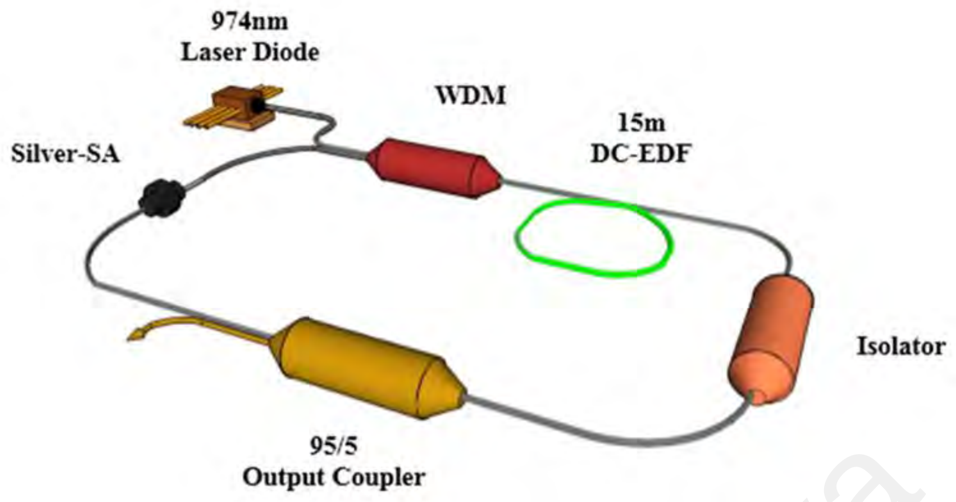

Figure 4. 8: The schematic diagram to generate passive Q-switched fiber laser by incorporated silver-nanoparticles as a saturable absorber.

4.3.2 Performances of Q-switching operation at S-band region

The performances of passive Q-switched at S-band region wavelength is monitored. Self-starting Q-switched operation was obtained at 170 mW pump power. Figure 4.9 (a)-(d) show the characteristics of the Q-switched operation when pump power was 260 mW. Figure 4.9(a) shows the optical spectrum with central wavelength, λc, at 1500 nm. The optical spectral broadening, evident from Figure 4.9(a) is due to Self-Phase Modulation (SPM). As shown in Figure 4.9(b), the time between pulses is 26 μs. At 170 mW, the pulse width is 4.8 μs at FHWM (Figure 4.9 (c). The signal-to-noise ratio (SNR) was measured using a RFSA with resolution bandwidth (RBW) of 300 Hz. The SNR is 35 dB, as shown in Figure 4.9 (d). When the frequency span was extended to 500 kHz, several frequency harmonics can be observed.

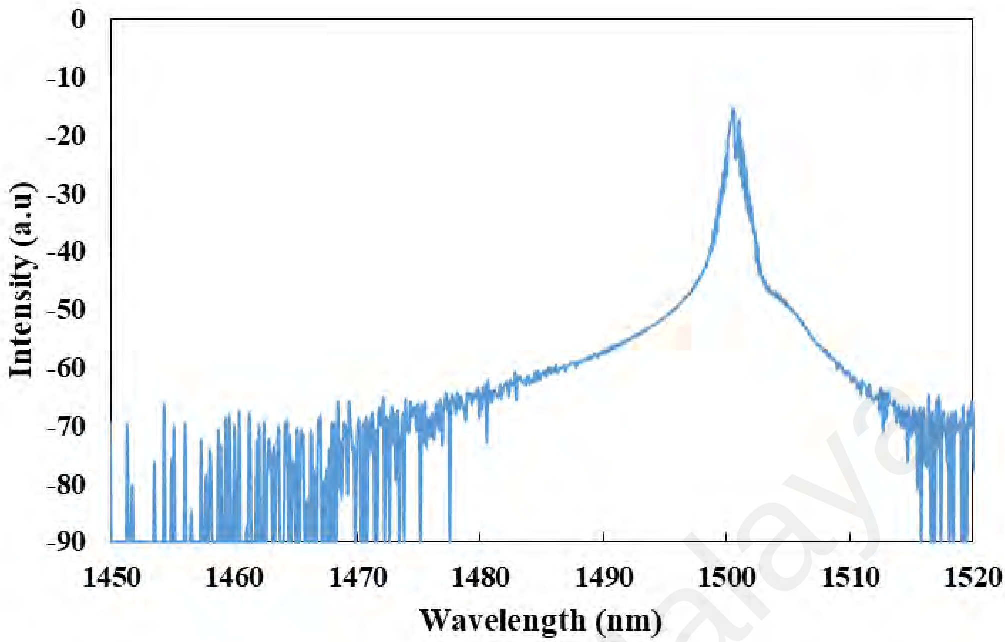
0
-10
-20
-30
-40
-50
-60
-70
-80
-90
Intensity (a.u)
1450
1460
1470
1480
1490
1500
1510
1520
Wavelength (nm)

(a)

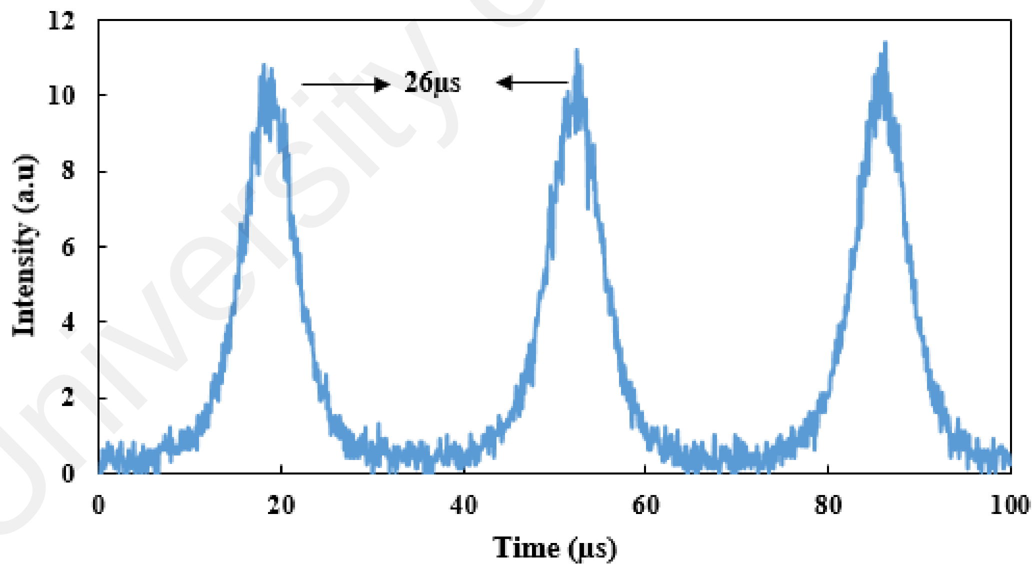
12
10
8
6
4
2
0
Intensity (a.u)
26μs
0
20
40
60
80
100
Time (μs)

(b)

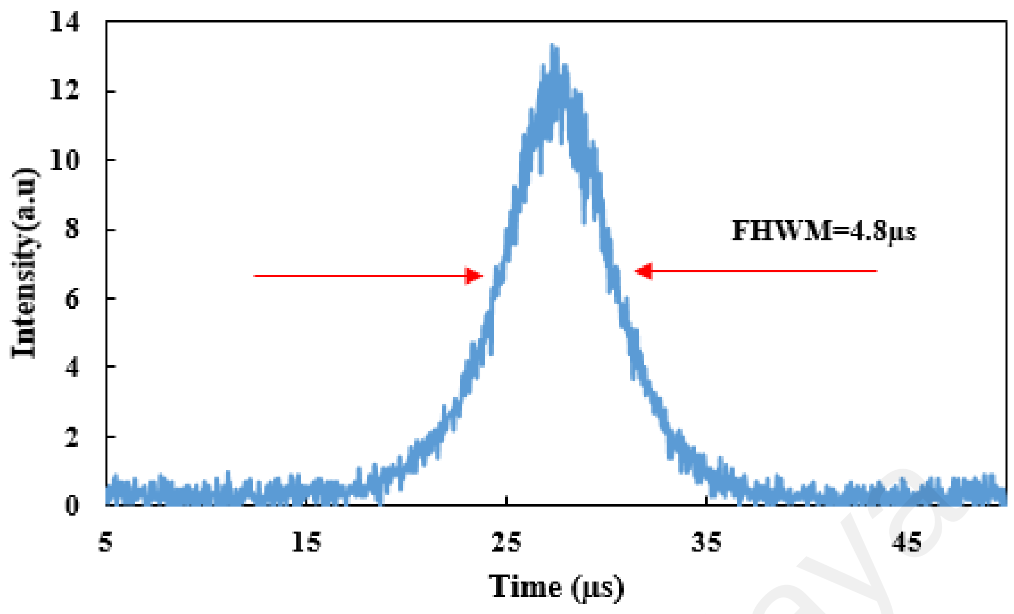

(c)

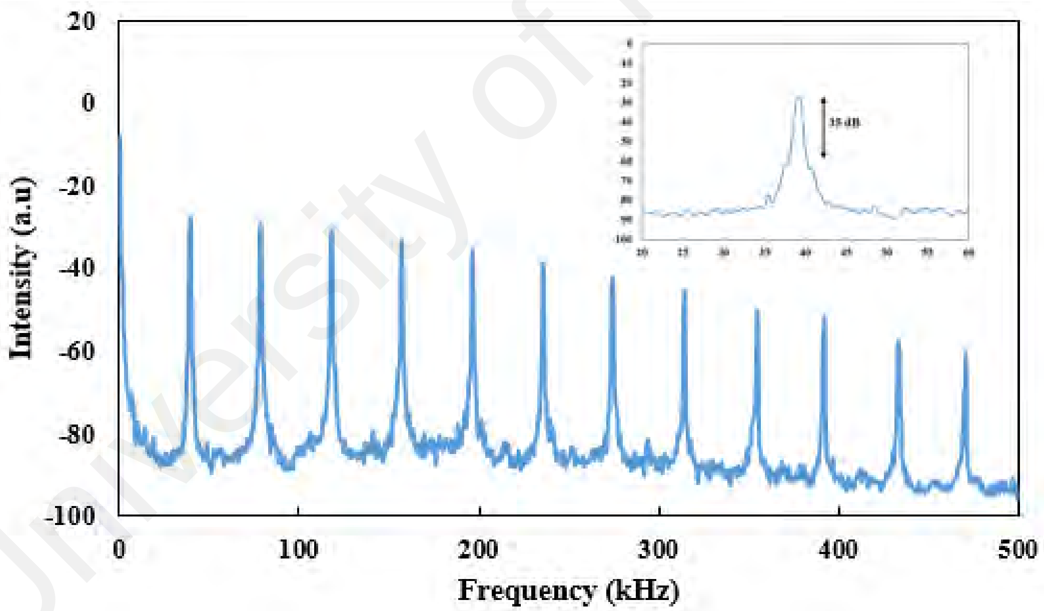

(d)

Figure 4. 9: The performance of silver-nanoparticles as SA in S-band region at 260 mW. (a) output of optical spectrum with central wavength of 1500 nm (b) oscilloscope traces with pulse duration of 26 μs (c) single pulse envelope with FHWM=4.8 μs and (d) RF output spectrum.

Figure 4.10 (a)-(c) represent the pulse width, repetition rate, peak power, pulse energy and output power against the pump power. Stable and self-starting Q-switched operation was attained (limited by the available pump power), ranging from 170 mW to 380 mW. The repetition rate increased gradually from 29 kHz to 48 kHz while the pulsewidth decreases from 6.8 μs to 0.8 μs, as shown in figure 4.10 (a). This presents a typical characteristic of passively Q-switched operation. From the plotted data in figure 4.10(b), the maximum pulse energy and peak power are 3 nJ and 4 mW, respectively. Figure 4.10(c) displays the output power which increased from 0.04 mW to 0.14 mW when the pump power increased from 170 mW to 380 mW.

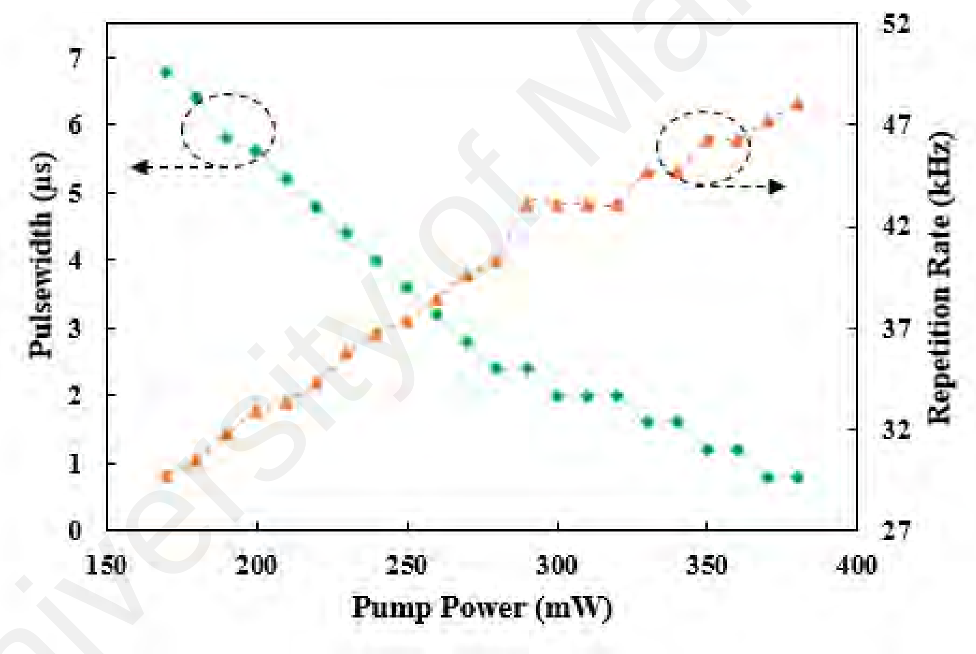

(a)

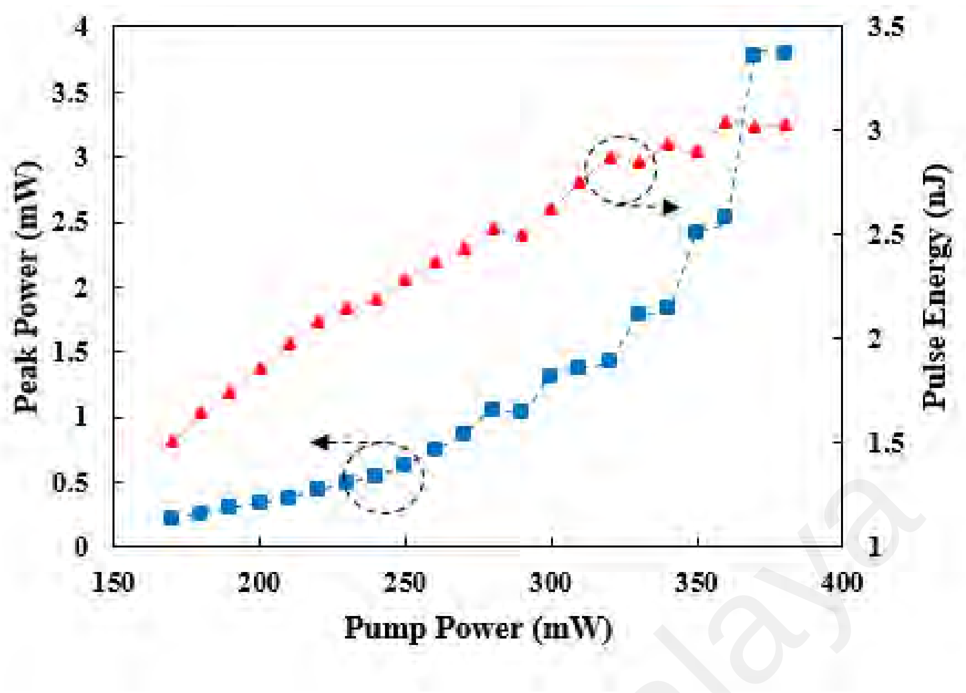

(b)

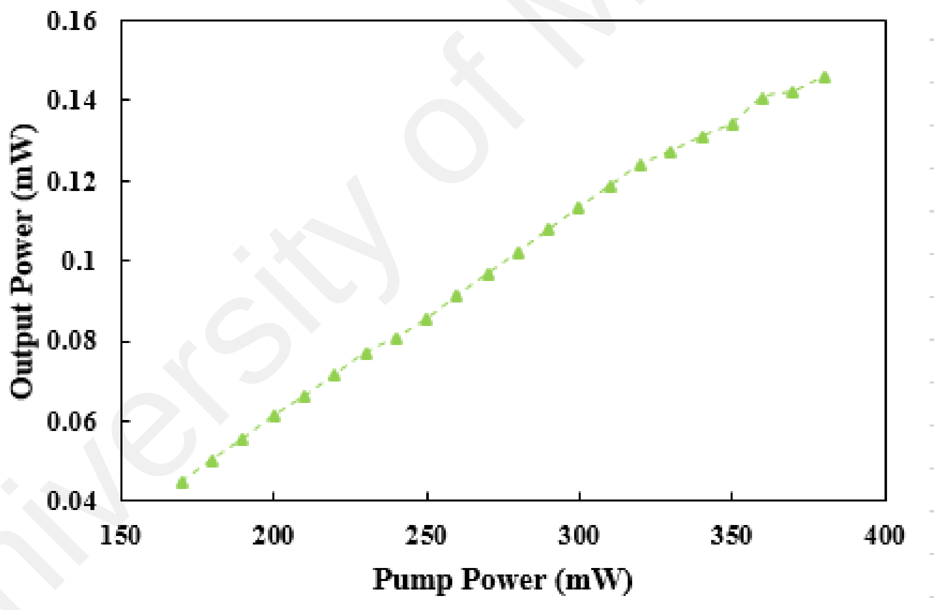

(c)

Figure 4. 10: (a) Pulsewidth and pulse repetition rate (b) pulse energy and peak power (c) measured output power as a function of pump power respectively.

4.3.3 Tuning range Characteristic at S-band region wavelength based Silver-nanoparticles as saturaber absorber.

To investigate the broadband wavelength tunability SNPs-SA using DC-EDF as gain medium at S-band region wavelength, the TBPF is incorporated into laser cavity system. The various spectra by tuning TBPF are represent in figure 4.11. At first, the TBPF is set at 1494nm, which is the peak emission of DC-EDF. The output wavelength can be varied from 1493nm to 1500nm that cover S-band region.

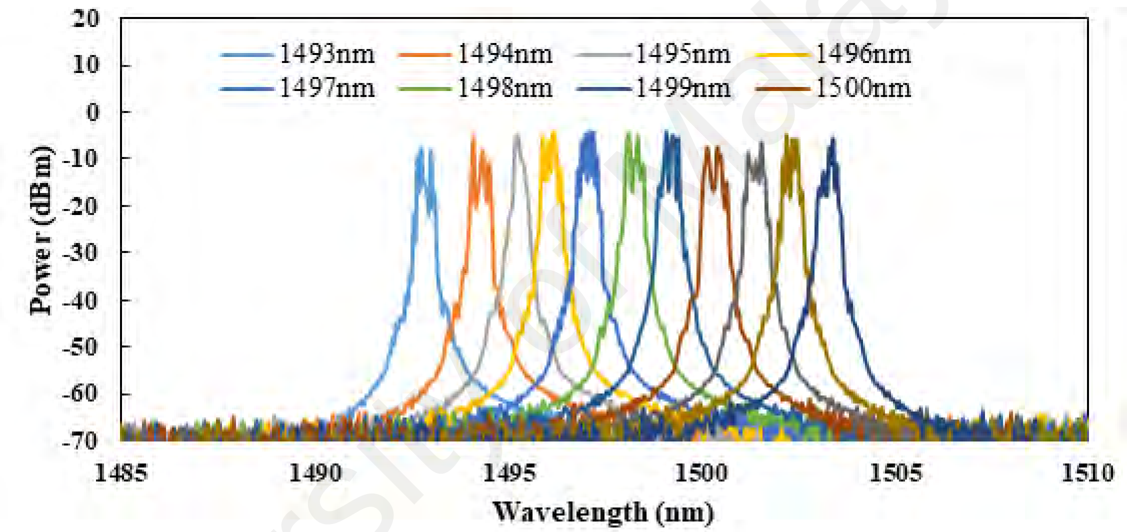

Figure 4. 11: The wavelength tunability of the Q-switched fiber lasers using SNPs SA at C-band region.

CHAPTER 5: CONCLUSON AND RECOMMENDATIONS

5.1 Conclusion

In this work, all the objectives that have been described in chapter 2 are achieved.

5.1.1 The optical properties of SNPs based SA

As mention in chapter 2, the first objective to characterize the silver-nanoparticle film as SA using Raman Spectroscopy is described in chapter 3. The raman spectrum of the silver nanoparticle SA exhibits two intensity peaks of MTMS monomer and MTMS-based cubic crystals at 248, 2912 and 2979 cm^{-1} which can be assigned to C-H stretching vibrations from methyl and methoxy groups in silane monomer originates from host material. The strong band in the range of 1300cm^{-1} to 1700 cm^{-1} at intensity peaks at 1385 cm^{-1} and 1588cm^{-1} are corresponding to Ag-O stretching and deformation vibration, respectively. Therefore, it is confirmed the SNPs are exist in the thin film.

Besides that, an experiment had been carried out to measure the nonlinear absorption properties of SNPs-based SA such a modulation depth and saturation intensity. From the experiment, the modulation depth and saturation intensity of the SNPs-based SA are calculated to be 31.6% and 0.54 $MWcm^2$.

5.1.2 The design the laser cavity and generation of Q-switched pulses at C- and S–bands region wavelength.

Ring cavity laser system using EDF and DC-EDF as gain medium to generate passive Q-switched laser at C- and S- band region wavelength is demonstrated by incorporating a SNPs-based SA. The SA introduced in the thin-film formed and sandwiching between fiber ferrules before integrated into ring cavity laser system which act as Q-switcher. The characteristic of Q-switched laser such as pulse width, repetition rate, average output power, pulse energy and output power as function to pump power at various operating wavelength which are C- and S-band are measured.

At C-band region wavelength, stable self-starting Q-switched laser with central wavelength of 1558.7nm is achieved. The repetition rate risingfrom 19.4 kHz to 74.1 kHz with the pulse duration become shortening from 8.88 – 3.2μs as the pump power increases from 20-260 mW. The wavelength can be varied from 1552.9 to 1580nm. The highest pulse energy and peak power are 8.17nJ and 2.55mW.

Meanwhile for the generation passive Q-switched at S-band region, A DC-EDF was utilized as gain medium in-order to shift the emission from C-band to S-band. The Q-switch operation began at 170 mW and last until 380 mW. The repetition rate rising from 29 kHz to 48 kHz with pulse width decreased from 6.8 μs to 0.8 μs. The maximum pulse energy and peak power are calculated to be 3 nJ and 4 mW, respectively.The wavelength can be tuned from 1493nm to 1500nm. Based on the presented results, SNPs can be used as a saturable absorber that can be utilized in various fiber laser cavity.

5.2 Future work

This section suggests a few recommendation that can be used for future work to improve the performances of SNPs as SA to generate passive Q-switched pulses. The recommendations are as follows:

1. To fabricate the SNPs film at different concentration.

The performances of passive Q-switched laser is depend on the performances of SA itself. To improve the performances of the Q-switched operation, the SA should be tested at some different concentration, examples at 1%, 2%, 3%, 4% or higher. Then we can choose among the tested sample that gives the best performances which could produce high peak power and pulse energy.

2. Pulse generation of SNPs can be further investigated to mode-locking and supercontinuum operation.

The laser cavity system can be enhance with a better control of laser cavity dispersion and also the nonlinear effect which can be contributed to generation more powerful pulses such as mode-locking and super-continuum.

3. To generate higher pulse energy of Q-switched pulses by using higher absorption of EDF.

High dopant concentration in EDF can increase the pump absorption which gives higher gain due to larger population inversion. Thus, the cavity length can be shorten since employing EDF with higher dopant concentration which also can reduced loss in cavity system. This will result high output power and generate high pulse energy.

REFERENCES

Agrawal, G. P. (1997). *Frontmatter and Index*: Wiley Online Library.

Ahmad, H., Ismail, M., Sathiyan, S., Reduan, S., Ruslan, N., Lee, C., . . . Harun, S. (2017). S-band Q-switched fiber laser using MoSe 2 saturable absorber. *Optics Communications, 382*, 93-98.

Ahmad, H., Ismail, M. A., Suthaskumar, M., Tiu, Z. C., Harun, S. W., Zulkifli, M. Z., . . . Sivaraj, S. (2016). S-band Q-switched fiber laser using molybdenum disulfide (MoS2) saturable absorber. *Laser Physics Letters, 13*(3), 035103. doi:10.1088/1612-2011/13/3/035103

Ahmad, H., Ruslan, N., Ali, Z., Reduan, S., Lee, C., Shaharuddin, R., . . . Ismail, M. (2016). Ag-nanoparticle as a Q switched device for tunable C-band fiber laser. *Optics Communications, 381*, 85-90.

Ahmad, H., Ruslan, N., Ismail, M., Ali, Z., Reduan, S., Lee, C., & Harun, S. (2016). Silver nanoparticle-film based saturable absorber for passively Q-switched erbium-doped fiber laser (EDFL) in ring cavity configuration. *Laser Physics, 26*(9), 095103.

Ahmad, H., Saat, N., & Harun, S. (2005). S-band erbium-doped fiber ring laser using a fiber Bragg grating. *Laser Physics Letters, 2*(7), 369.

Ahmad, H., Samion, M., Muhamad, A., Sharbirin, A., & Ismail, M. (2016). Passively Q-switched thulium-doped fiber laser with silver-nanoparticle film as the saturable absorber for operation at 2.0 µm. *Laser Physics Letters, 13*(12), 126201.

Ahmad, H., Soltanian, M., Narimani, L., Amiri, I., Khodaei, A., & Harun, S. (2015). Tunable S-band Q-switched fiber laser using Bi 2 Se 3 as the saturable absorber. *IEEE Photonics Journal, 7*(3), 1-8.

Ahmad, H., Zulkifli, M., Muhammad, F., Zulkifli, A., & Harun, S. (2013). Tunable graphene-based Q-switched erbium-doped fiber laser using fiber Bragg grating. *Journal of Modern Optics, 60*(3), 202-212.

Ajayan, P., & Lijima, S. (1992). Smallest carbon nanotube. *Nature, 358*, 23.

Alivisatos, A. P. (1996). Semiconductor clusters, nanocrystals, and quantum dots. *Science, 271*(5251), 933.

Antonio-Lopez, J., Castillo-Guzman, A., May-Arrioja, D., Selvas-Aguilar, R., & LiKamWa, P. (2010). Tunable multimode-interference bandpass fiber filter. *Optics letters, 35*(3), 324-326.

Arbore, M. A., & Keaton, G. L. (2005). Fiber amplifiers with depressed cladding and their uses in Er-doped fiber amplifiers for the S-band: Google Patents.

Bao, Q., Zhang, H., Ni, Z., Wang, Y., Polavarapu, L., Shen, Z., . . . Loh, K. P. (2011). Monolayer graphene as a saturable absorber in a mode-locked laser. *Nano Research, 4*(3), 297-307.

Bao, Q., Zhang, H., Wang, Y., Ni, Z., Yan, Y., Shen, Z. X., . . . Tang, D. Y. (2009). Atomic-Layer Graphene as a Saturable Absorber for Ultrafast Pulsed Lasers. *Advanced Functional Materials, 19*(19), 3077-3083. doi:10.1002/adfm.200901007

Brunner, T. A., & Moore, G. E. (1995). Lithography and the future of Moore's Law. *2440*, 2-17. doi:10.1117/12.209244

Chen, B., Zhang, X., Wu, K., Wang, H., Wang, J., & Chen, J. (2015). Q-switched fiber laser based on transition metal dichalcogenides MoS2, MoSe2, WS2, and WSe2. *Optics Express, 23*(20), 26723-26737. doi:10.1364/OE.23.026723

Chen, F., Cheng, J., Dai, S., Xu, Z., Ji, W., Tan, R., & Zhang, Q. (2014). Third-order optical nonlinearity at 800 and 1300 nm in bismuthate glasses doped with silver nanoparticles. *Optics Express, 22*(11), 13438-13447.

Chen, N.-K., Chi, S., & Tseng, S.-M. (2005). An efficient local fundamental-mode cutoff for thermo-optic tunable Er 3+-doped fiber ring laser. *Optics Express, 13*(18), 7250-7255.

Chen, Y., Jiang, G., Chen, S., Guo, Z., Yu, X., Zhao, C., . . . Tang, D. (2015). Mechanically exfoliated black phosphorus as a new saturable absorber for both Q-switching and mode-locking laser operation. *Optics Express, 23*(10), 12823-12833.

Chen, Y., Zhao, C., Chen, S., Du, J., Tang, P., Jiang, G., . . . Tang, D. (2014). Large energy, wavelength widely tunable, topological insulator Q-switched erbium-doped fiber laser. *IEEE Journal of Selected Topics in Quantum Electronics, 20*(5), 315-322.

Cheng, H. P. H., Tidemand-Lichtenberg, P., Jensen, O. B., Andersen, P. E., Petersen, P. M., & Pedersen, C. (2010). All passive synchronized Q-switching of a quasi-three-level and a four-level Nd: YAG laser. *Optics Express, 18*(23), 23987-23993.

Coleman, J. N., Lotya, M., O'Neill, A., Bergin, S. D., King, P. J., Khan, U., . . . Smith, R. J. (2011). Two-dimensional nanosheets produced by liquid exfoliation of layered materials. *Science, 331*(6017), 568-571.

Collins, R., & Kisliuk, P. (1962). Control of population inversion in pulsed optical masers by feedback modulation. *Journal of Applied Physics, 33*(6), 2009-2011.

Creighton, J. A., Blatchford, C. G., & Albrecht, M. G. (1979). Plasma resonance enhancement of Raman scattering by pyridine adsorbed on silver or gold sol particles of size comparable to the excitation wavelength. *Journal of the Chemical Society, Faraday Transactions 2: Molecular and Chemical Physics, 75*, 790-798.

Csele, M. (2011). *Fundamentals of light sources and lasers*: John Wiley & Sons.

Degnan, J. J. (1995). Optimization of passively Q-switched lasers. *IEEE Journal of Quantum Electronics, 31*(11), 1890-1901.

Delgado-Pinar, M., Zalvidea, D., Diez, A., Pérez-Millán, P., & Andrés, M. (2006). Q-switching of an all-fiber laser by acousto-optic modulation of a fiber Bragg grating. *Optics Express, 14*(3), 1106-1112.

Desurvire, E., & Simpson, J. R. (1989). Amplification of spontaneous emission in erbium-doped single-mode fibers. *JOURNAL OF LIGHTWAVE TECHNOLOGY, 7*(5), 835-845. doi:10.1109/50.19124

Digonnet, M. J. (1993). Theory of operation of laser fiber devices. *OPTICAL ENGINEERING-NEW YORK-MARCEL DEKKER INCORPORATED-, 37*, 181-181.

Dong, B., Hao, J., Liaw, C.-y., Lin, B., & Tjin, S. C. (2010). Simultaneous strain and temperature measurement using a compact photonic crystal fiber inter-modal interferometer and a fiber Bragg grating. *Applied Optics, 49*(32), 6232-6235.

Dong, B., Hu, J., Liaw, C.-Y., Hao, J., & Yu, C. (2011). Wideband-tunable nanotube Q-switched low threshold erbium doped fiber laser. *Applied Optics, 50*(10), 1442-1445.

El-Sayed, M. A. (2001). Some interesting properties of metals confined in time and nanometer space of different shapes. *Accounts of Chemical Research, 34*(4), 257-264.

El-Sherif, A. F., & King, T. A. (2003). High-energy, high-brightness Q-switched Tm 3+-doped fiber laser using an electro-optic modulator. *Optics Communications, 218*(4), 337-344.

Ellingson, R. J., Beard, M. C., Johnson, J. C., Yu, P., Micic, O. I., Nozik, A. J., . . . Efros, A. L. (2005). Highly efficient multiple exciton generation in colloidal PbSe and PbS quantum dots. *Nano letters, 5*(5), 865-871.

Fan, Y.-X., He, J.-L., Wang, Y.-G., Liu, S., Wang, H.-T., & Ma, X.-Y. (2005). 2-ps passively mode-locked Nd: YVO 4 laser using an output-coupling-type semiconductor saturable absorber mirror. *Applied Physics Letters, 86*(10), 101103.

Faraday, M. (1857). The Bakerian lecture: experimental relations of gold (and other metals) to light. *Philosophical Transactions of the Royal Society of London, 147*, 145-181.

Foroni, M., Poli, F., Cucinotta, A., & Selleri, S. (2006). S-band depressed-cladding erbium-doped fiber amplifier with double-pass configuration. *Optics letters, 31*(22), 3228-3230.

Franklin, A. D. (2015). DEVICE TECHNOLOGY. Nanomaterials in transistors: From high-performance to thin-film applications. *Science, 349*(6249), aab2750. doi:10.1126/science.aab2750

Garmire, E. (2000). Resonant optical nonlinearities in semiconductors. *IEEE Journal of Selected Topics in Quantum Electronics, 6*(6), 1094-1110.

Gasaymeh, S. S., Radiman, S., Heng, L. Y., Saion, E., & Saeed, G. M. (2010). Synthesis and characterization of silver/polyvinilpirrolidone (Ag/PVP) nanoparticles using gamma irradiation techniques. *American Journal of Applied Sciences, 7*(7), 879-888.

Geim, A. K., & Novoselov, K. S. (2007). The rise of graphene. *Nature materials, 6*(3), 183-191.

Geist, F., Guyenot, M., Herbst, W., Pascher, H., Verkerk, R., & Prettl, W. (1997). Q-switched CO 2 laser with pulsed longitudinal discharge for nonlinear optical applications. *Review of scientific instruments, 68*(9), 3599-3600.

George, P. A., Strait, J., Dawlaty, J., Shivaraman, S., Chandrashekhar, M., Rana, F., & Spencer, M. G. (2008). Ultrafast optical-pump terahertz-probe spectroscopy of the carrier relaxation and recombination dynamics in epitaxial graphene. *arXiv preprint arXiv:0805.4647*.

Glubokov, D. A. e., Sychev, V. V. e., Mikhailov, A. S., Korolkov, A. E. e., Chubich, D. A. e., Shapiro, B. I., & Vitukhnovskii, A. G. e. (2014). Saturable absorber based on silver nanoparticles for passively mode-locked lasers. *Quantum Electronics, 44*(4), 314.

Gordon, J. P., & Haus, H. A. (1986). Random walk of coherently amplified solitons in optical fiber transmission. *Optics letters, 11*(10), 665-667.

Gouveia-Neto, A., Gomes, A., & Taylor, J. (1988). Soliton Raman fibre-ring oscillators. *Optical and quantum electronics, 20*(2), 165-174.

Gräf, S., Staupendahl, G., Krämer, A., & Müller, F. A. (2015). High precision materials processing using a novel Q-switched CO2 laser. *Optics and Lasers in Engineering, 66*, 152-157.

Guo, B., Yao, Y., Yang, Y.-F., Yuan, Y.-J., Wang, R.-L., Wang, S.-G., . . . Yan, B. (2015). Topological insulator: Bi2Se3/polyvinyl alcohol film-assisted multi-wavelength ultrafast erbium-doped fiber laser. *Journal of Applied Physics, 117*(6), 063108.

Guo, H., Feng, M., Song, F., Li, H., Ren, A., Wei, X., . . . Tian, J. (2016). $ Q $-Switched Erbium-Doped Fiber Laser Based on Silver Nanoparticles as a Saturable Absorber. *IEEE Photonics Technology Letters, 28*(2), 135-138.

Han, M., Zhang, S., Li, X., Zhang, H., Wen, F., & Yang, Z. (2014). High-energy, tunable-wavelengths, Q-switched pulse laser. *Optics Communications, 326*, 24-28.

He, G. S., Markowicz, P. P., Lin, T.-C., & Prasad, P. N. (2002). Observation of stimulated emission by direct three-photon excitation. *Nature, 415*(6873), 767-770.

He, J.-L., Fan, Y.-X., Du, J., Wang, Y.-G., Liu, S., Wang, H.-T., . . . Hang, Y. (2004). 4-ps passively mode-locked Nd: Gd 0.5 Y 0.5 VO 4 laser with a semiconductor saturable-absorber mirror. *Optics letters, 29*(23), 2803-2805.

Hellwarth, R. (1961). Advances in quantum electronics: Columbia Press, New York.

Henglein, A. (1989). Small-particle research: physicochemical properties of extremely small colloidal metal and semiconductor particles. *Chemical Reviews, 89*(8), 1861-1873.

Hill, K., Johnson, D., Kawasaki, B., & MacDonald, R. (1978). cw three-wave mixing in single-mode optical fibers. *Journal of Applied Physics, 49*(10), 5098-5106.

Iga, M., Seki, A., & Watanabe, K. (2004). Hetero-core structured fiber optic surface plasmon resonance sensor with silver film. *Sensors and Actuators B: Chemical, 101*(3), 368-372.

Ippen, E., & Stolen, R. (1972). Stimulated Brillouin scattering in optical fibers. *Applied Physics Letters, 21*(11), 539-541.

Islam, M. N., Simpson, J., Shang, H., Mollenauer, L., & Stolen, R. (1987). Amplifier/compressor fiber Raman lasers. *Optics letters, 12*(10), 814-816.

Jin, R., Cao, Y., Mirkin, C. A., Kelly, K., Schatz, G. C., & Zheng, J. (2001). Photoinduced conversion of silver nanospheres to nanoprisms. *Science, 294*(5548), 1901-1903.

Jin, R., Cao, Y. C., Hao, E., Métraux, G. S., Schatz, G. C., & Mirkin, C. A. (2003). Controlling anisotropic nanoparticle growth through plasmon excitation. *Nature, 425*(6957), 487-490.

Jung, C. Y., Kim, H. S., Hah, H. J., & Koo, S. M. (2009). Self-assembly growth process for polyhedral oligomeric silsesquioxane cubic crystals. *Chemical Communications*(10), 1219-1221.

Kafka, J., & Baer, T. (1987). Fiber Raman soliton laser pumped by a Nd: YAG laser. *Optics letters, 12*(3), 181-183.

Kao, K., & Hockham, G. A. (1966). *Dielectric-fibre surface waveguides for optical frequencies.* Paper presented at the Proceedings of the Institution of Electrical Engineers.

Kapany, N. (1967). Fiber optics. Principles and applications. *New York: Academic Press, 1967*.

Kapron, F., Keck, D., & Maurer, R. (1970). Radiation losses in glass optical waveguides. *Applied Physics Letters, 17*(10), 423-425.

Kashiwagi, K., & Yamashita, S. (2010). Optical Deposition of Carbon Nanotubes for Fiber-based Device Fabrication. In B. Pal (Ed.), *Frontiers in Guided Wave Optics and Optoelectronics* (pp. Ch. 19). Rijeka: InTech.

Kassani, S. H., Khazaeinezhad, R., Jeong, H., Nazari, T., Yeom, D.-I., & Oh, K. (2015). All-fiber Er-doped Q-Switched laser based on Tungsten Disulfide saturable absorber. *Optical Materials Express, 5*(2), 373. doi:10.1364/ome.5.000373

Keller, U., Weingarten, K. J., Kartner, F. X., Kopf, D., Braun, B., Jung, I. D., . . . Der Au, J. A. (1996). Semiconductor saturable absorber mirrors (SESAM's) for femtosecond to nanosecond pulse generation in solid-state lasers. *IEEE Journal of Selected Topics in Quantum Electronics, 2*(3), 435-453.

Kelly, K. L., Coronado, E., Zhao, L. L., & Schatz, G. C. (2003). The optical properties of metal nanoparticles: the influence of size, shape, and dielectric environment. *Journal of Physical Chemistry B-Condensed Phase, 107*(3), 668-677.

Kilpelä, A., Pennala, R., & Kostamovaara, J. (2001). Precise pulsed time-of-flight laser range finder for industrial distance measurements. *Review of scientific instruments, 72*(4), 2197-2202.

Kim, K.-H., Husakou, A., & Herrmann, J. (2010). Saturable absorption in composites doped with metal nanoparticles. *Optics Express, 18*(21), 21918-21925.

Koechner, W. (2006). Q-Switching *Solid-State Laser Engineering* (pp. 488-533). New York, NY: Springer New York.

Koechner, W. (2013). *Solid-state laser engineering* (Vol. 1): Springer.

Kölbl, J., Fröschl, M., Seedsman, A., & Sperber, P. (2008). *Near-infrared laser range finder using kHz repetition rate.* Paper presented at the SPIE Europe Security and Defence.

Kumar, H., & Rani, R. (2013). Structural characterization of silver nanoparticles synthesized by micro emulsion route. *Int. J. Eng. Innovative Technol., 3*.

Kuzmenko, A., Van Heumen, E., Carbone, F., & Van Der Marel, D. (2008). Universal optical conductance of graphite. *Physical Review Letters, 100*(11), 117401.

Laroche, M., Chardon, A., Nilsson, J., Shepherd, D., Clarkson, W., Girard, S., & Moncorgé, R. (2002). Compact diode-pumped passively Q-switched tunable Er–Yb double-clad fiber laser. *Optics letters, 27*(22), 1980-1982.

Lee, P., & Meisel, D. (1982). Adsorption and surface-enhanced Raman of dyes on silver and gold sols. *J. Phys. Chem, 86*(17), 3391-3395.

Li, H., Xia, H., Lan, C., Li, C., Zhang, X., Li, J., & Liu, Y. (2015). Passively $ Q $-switched erbium-doped fiber laser based on few-layer MoS 2 saturable absorber. *IEEE Photonics Technology Letters, 27*(1), 69-72.

Liu, J., Xu, J., & Wang, P. (2012). Graphene-based passively Q-switched 2µm thulium-doped fiber laser. *Optics Communications, 285*(24), 5319-5322. doi:10.1016/j.optcom.2012.07.063

Liu, S., Huang, W., Chen, S., Avivi, S., & Gedanken, A. (2001). Synthesis of X-ray amorphous silver nanoparticles by the pulse sonoelectrochemical method. *Journal of non-crystalline solids, 283*(1), 231-236.

Lu, Y., Liu, G. L., & Lee, L. P. (2005). High-density silver nanoparticle film with temperature-controllable interparticle spacing for a tunable surface enhanced Raman scattering substrate. *Nano letters, 5*(1), 5-10.

Luo, A.-P., Luo, Z.-C., & Xu, W.-C. (2009). Tunable and switchable multiwavelength erbium-doped fiber ring laser based on a modified dual-pass Mach-Zehnder interferometer. *Optics letters, 34*(14), 2135-2137.

Luo, Z., Huang, Y., Zhong, M., Li, Y., Wu, J., Xu, B., . . . Weng, J. (2014). 1-, 1.5-, and 2-µm fiber lasers Q-switched by a broadband few-layer MoS 2 saturable absorber. *JOURNAL OF LIGHTWAVE TECHNOLOGY, 32*(24), 4077-4084.

Maciel, G., Rakov, N., de Araujo, C. B., Lipovskii, A., & Tagantsev, D. (2001). Optical limiting behavior of a glass–ceramic containing sodium niobate crystallites. *Applied Physics Letters, 79*(5), 584-586.

Maier, S. A., Brongersma, M. L., Kik, P. G., Meltzer, S., Requicha, A. A., & Atwater, H. A. (2001). Plasmonics—a route to nanoscale optical devices. *Advanced Materials, 13*(19), 1501-1505.

Maillard, M., Giorgio, S., & Pileni, M.-P. (2002). Silver nanodisks. *Advanced Materials, 14*(15), 1084.

Maiman, T. H. (1960). Stimulated Optical Radiation in Ruby. *Nature, 187*(4736), 493-494.

Markovich, G., Collier, C. P., Henrichs, S. E., Remacle, F., Levine, R. D., & Heath, J. R. (1999). Architectonic quantum dot solids. *Accounts of Chemical Research, 32*(5), 415-424.

McClung, F., & Hellwarth, R. (1962). Giant optical pulsations from ruby. *Applied Optics, 1*(101), 103-105.

Michelangeli, G. B., Giuliani, G., Palange, E., & Penco, E. (1986). Q switching and cavity dumping of a high-power cw Nd: YAG laser by means of a novel electro-optic configuration. *Optics letters, 11*(6), 360-362.

Mie, G. (1976). Contributions to the optics of turbid media, particularly of colloidal metal solutions. *Contributions to the optics of turbid media, particularly of colloidal metal solutions Transl. into ENGLISH from Ann. Phys.(Leipzig), v. 25, no. 3, 1908 p 377-445, 1*, 377-445.

Miya, T., Terunuma, Y., Hosaka, T., & Miyashita, T. (1979). Ultimate low-loss single-mode fibre at 1.55 µm. *Electronics Letters, 15*(4), 106-108.

Mollenauer, L., Gordon, J., Mamyshev, P., Kaminow, I., & Koch, T. (1997). Optical Fiber Telecommunications IIIA: Academic Press, San Diego.

Mollenauer, L. F., & Stolen, R. H. (1984). The soliton laser. *Optics letters, 9*(1), 13-15.

Moskovits, M., & Suh, J. (1984). Surface selection rules for surface-enhanced Raman spectroscopy: calculations and application to the surface-enhanced Raman spectrum of phthalazine on silver. *The Journal of Physical Chemistry, 88*(23), 5526-5530.

Mulvaney, P. (1996). Surface plasmon spectroscopy of nanosized metal particles. *Langmuir, 12*(3), 788-800.

Murray, C., Sun, S., Doyle, H., & Betley, T. (2001). Monodisperse 3d transition-metal (Co, Ni, Fe) nanoparticles and their assembly intonanoparticle superlattices. *Mrs Bulletin, 26*(12), 985-991.

Nakatsuka, H., Grischkowsky, D., & Balant, A. (1981). Nonlinear picosecond-pulse propagation through optical fibers with positive group velocity dispersion. *Physical Review Letters, 47*(13), 910.

Nelson, L., Jones, D., Tamura, K., Haus, H., & Ippen, E. (1997). Ultrashort-pulse fiber ring lasers. *Applied Physics B: Lasers and Optics, 65*(2), 277-294.

Nicewarner-Pena, S. R., Freeman, R. G., Reiss, B. D., He, L., Peña, D. J., Walton, I. D., . . . Natan, M. J. (2001). Submicrometer metallic barcodes. *Science, 294*(5540), 137-141.

Nie, S., & Emory, S. R. (1997). Probing single molecules and single nanoparticles by surface-enhanced Raman scattering. *Science, 275*(5303), 1102-1106.

Nikolaus, B., & Grischkowsky, D. (1983). 90-fs tunable optical pulses obtained by two-stage pulse compression. *Applied Physics Letters, 43*(3), 228-230.

Nissilae, S. M., & Kostamovaara, J. T. (1993). *Fiber laser as the pulse source for a laser rangefinder system.* Paper presented at the Industrial Applications of Optical Inspection, Metrology, and Sensing.

Novoselov, K. S., Jiang, D., Schedin, F., Booth, T. J., Khotkevich, V. V., Morozov, S. V., & Geim, A. K. (2005). Two-dimensional atomic crystals. *Proc Natl Acad Sci U S A, 102*(30), 10451-10453. doi:10.1073/pnas.0502848102

Okhotnikov, O., Grudinin, A., & Pessa, M. (2004). Ultra-fast fibre laser systems based on SESAM technology: new horizons and applications. *New journal of physics, 6*(1), 177.

Pal, A., Shah, S., & Devi, S. (2007). Preparation of silver, gold and silver–gold bimetallic nanoparticles in w/o microemulsion containing TritonX-100. *Colloids and Surfaces A: Physicochemical and Engineering Aspects, 302*(1), 483-487.

Patel, K., Kapoor, S., Dave, D. P., & Mukherjee, T. (2005). Synthesis of nanosized silver colloids by microwave dielectric heating. *Journal of Chemical Sciences, 117*(1), 53-60.

Pileni, M. P. (2001). Magnetic fluids: fabrication, magnetic properties, and organization of nanocrystals. *Advanced Functional Materials, 11*(5), 323-336.

Pillai, Z. S., & Kamat, P. V. (2004). What factors control the size and shape of silver nanoparticles in the citrate ion reduction method? *The Journal of Physical Chemistry B, 108*(3), 945-951.

Popa, D., Sun, Z., Hasan, T., Torrisi, F., Wang, F., & Ferrari, A. (2011). Graphene Q-switched, tunable fiber laser. *Applied Physics Letters, 98*(7), 073106.

Qi, Y., Zhou, Y., Wu, L., Yang, F., Peng, S., Zheng, S., & Yin, D. (2014). Silver nanoparticles enhanced 1.53 µm band fluorescence of Er 3+/Yb 3+ codoped tellurite glasses. *Journal of Luminescence, 153*, 401-407.

Qin-Yong, Z., Yong, W., Ji-Chuan, X., & Da-Yong, Z. (2011). Modeling the pulse shape of Q-switched lasers to account for terminal-level relaxation. *Chinese Physics B, 20*(3), 034204.

Ramaswami, R., Sivarajan, K., & Sasaki, G. (2009). *Optical networks: a practical perspective*: Morgan Kaufmann.

Reifler, E., Nuhfer, N., & Towe, E. (2014). Structure and optical properties of some layered two-dimensional transition-metal dichalcogenides: molybdenum disulfide, molybdenum diselenide, and tungsten diselenide. *Microscopy and Microanalysis, 20*(S3), 1752-1753.

Reinhard, B. M., Siu, M., Agarwal, H., Alivisatos, A. P., & Liphardt, J. (2005). Calibration of dynamic molecular rulers based on plasmon coupling between gold nanoparticles. *Nano letters, 5*(11), 2246-2252.

Renk, K. F. (2012). *Basics of laser physics*: Springer.

Rosemary, M., & Pradeep, T. (2003). Solvothermal synthesis of silver nanoparticles from thiolates. *Journal of colloid and interface science, 268*(1), 81-84.

Rosolem, J., Juriollo, A., Arradi, R., Coral, A., Oliveira, J., & Romero, M. A. (2005). All silica S-band double-pass erbium-doped fiber amplifier. *IEEE Photonics Technology Letters, 17*(7), 1399-1401.

Rudenko, A. N., & Katsnelson, M. I. (2014). Quasiparticle band structure and tight-binding model for single-and bilayer black phosphorus. *Physical Review B, 89*(20), 201408.

Rustad, L. (2001). Global change: Matter of time on the prairie. *Nature, 413*(6856), 578-579.

Salkar, R., Jeevanandam, P., Aruna, S., Koltypin, Y., & Gedanken, A. (1999). The sonochemical preparation of amorphous silver nanoparticles. *Journal of Materials Chemistry, 9*(6), 1333-1335.

Schaller, R. R. (1997). Moore's law: past, present and future. *IEEE Spectrum, 34*(6), 52-59. doi:10.1109/6.591665

Schawlow, A. L., & Townes, C. H. (1958). Infrared and optical masers. *Physical Review, 112*(6), 1940.

Schultz, S., Smith, D. R., Mock, J. J., & Schultz, D. A. (2000). Single-target molecule detection with nonbleaching multicolor optical immunolabels. *Proceedings of the National Academy of Sciences, 97*(3), 996-1001.

Shank, C., Fork, R., Yen, R., Stolen, R., & Tomlinson, W. J. (1982). Compression of femtosecond optical pulses. *Applied Physics Letters, 40*(9), 761-763.

Singh, M., Singh, S., Prasad, S., & Gambhir, I. (2008). Nanotechnology in medicine and antibacterial effect of silver nanoparticles. *Digest Journal of Nanomaterials and Biostructures, 3*(3), 115-122.

Singh, V., & Aghamkar, P. (2014). Surface plasmon enhanced third-order optical nonlinearity of Ag nanocomposite film. *Applied Physics Letters, 104*(11), 111112.

Smith, R. G. (1972). Optical power handling capacity of low loss optical fibers as determined by stimulated Raman and Brillouin scattering. *Applied Optics, 11*(11), 2489-2494.

Soroushian, B., Lampre, I., Belloni, J., & Mostafavi, M. (2005). Radiolysis of silver ion solutions in ethylene glycol: solvated electron and radical scavenging yields. *Radiation Physics and Chemistry, 72*(2), 111-118.

Spühler, G., Paschotta, R., Fluck, R., Braun, B., Moser, M., Zhang, G., . . . Keller, U. (1999). Experimentally confirmed design guidelines for passively Q-switched microchip lasers using semiconductor saturable absorbers. *JOSA B, 16*(3), 376-388.

Starowicz, M., Stypuła, B., & Banaś, J. (2006). Electrochemical synthesis of silver nanoparticles. *Electrochemistry Communications, 8*(2), 227-230.

Stolen, R., & Ashkin, A. (1973). Optical Kerr effect in glass waveguide. *Applied Physics Letters, 22*(6), 294-296.

Stolen, R., Bjorkholm, J., & Ashkin, A. (1974). Phase-matched three-wave mixing in silica fiber optical waveguides. *Applied Physics Letters, 24*(7), 308-310.

Stolen, R. H., Ippen, E., & Tynes, A. (1972). Raman oscillation in glass optical waveguide. *Applied Physics Letters, 20*(2), 62-64.

Stöppler, G., Kieleck, C., & Eichhorn, M. (2010). *High-pulse energy Q-switched Tm3+: YAG laser for nonlinear frequency conversion to the mid-IR.* Paper presented at the Security+ Defence.

Sun, Z., Hasan, T., Torrisi, F., Popa, D., Privitera, G., Wang, F., . . . Ferrari, A. C. (2010). Graphene mode-locked ultrafast laser. *ACS Nano, 4*(2), 803-810. doi:10.1021/nn901703e

Svelto, O., & Hanna, D. C. (1998). Principles of lasers.

Taton, T. A., Mirkin, C. A., & Letsinger, R. L. (2000). Scanometric DNA array detection with nanoparticle probes. *Science, 289*(5485), 1757-1760.

Thyagarajan, K., & Kakkar, C. (2004). S-band single-stage EDFA with 25-dB gain using distributed ASE suppression. *IEEE Photonics Technology Letters, 16*(11), 2448-2450.

Van Dijk, M., Tchebotareva, A., Orrit, M., Lippitz, M., Berciaud, S., Lasne, D., . . . Lounis, B. (2006). Absorption and scattering microscopy of single metal nanoparticles. *Physical Chemistry Chemical Physics, 8*(30), 3486-3495.

Welford, D. (2003). Passively Q-switched lasers. *IEEE circuits and devices magazine, 19*(4), 31-36.

Woodward, R., Howe, R., Runcorn, T., Hu, G., Torrisi, F., Kelleher, E., & Hasan, T. (2015). Wideband saturable absorption in few-layer molybdenum diselenide (MoSe 2) for Q-switching Yb-, Er-and Tm-doped fiber lasers. *Optics Express, 23*(15), 20051-20061.

Woodward, R., Kelleher, E., Howe, R., Hu, G., Torrisi, F., Hasan, T., . . . Taylor, J. (2014). Tunable Q-switched fiber laser based on saturable edge-state absorption in few-layer molybdenum disulfide (MoS 2). *Optics Express, 22*(25), 31113-31122.

Wu, K., Zhang, X., Wang, J., Li, X., & Chen, J. (2015). WS 2 as a saturable absorber for ultrafast photonic applications of mode-locked and Q-switched lasers. *Optics Express, 23*(9), 11453-11461.

Xie, Y., Ye, R., & Liu, H. (2006). Synthesis of silver nanoparticles in reverse micelles stabilized by natural biosurfactant. *Colloids and Surfaces A: Physicochemical and Engineering Aspects, 279*(1), 175-178.

Yan, P., Chen, H., Yin, J., Xu, Z., Li, J., Jiang, Z., . . . Ruan, S. (2017). Large-area tungsten disulfide for ultrafast photonics. *Nanoscale*. doi:10.1039/c6nr09183k

Yeh, C.-H., Lee, C.-C., & Chi, S. (2004). 120-nm bandwidth erbium-doped fiber amplifier in parallel configuration. *IEEE Photonics Technology Letters, 16*(7), 1637-1639.

Yguerabide, J., & Yguerabide, E. E. (1998). Light-scattering submicroscopic particles as highly fluorescent analogs and their use as tracer labels in clinical and biological applications: I. Theory. *Analytical biochemistry, 262*(2), 137-156.

Yukna, J. (2007). *Computational and experimental investigations of the structural properties, electronic properties, and applications of silver, gold, mercury selenide, silver sulfide, and nickel sulfide nanoparticles*: Southern Illinois University at Carbondale.

Zhang, H., Liu, C.-X., Qi, X.-L., Dai, X., Fang, Z., & Zhang, S.-C. (2009). Topological insulators in Bi2Se3, Bi2Te3 and Sb2Te3 with a single Dirac cone on the surface. *Nature physics, 5*(6), 438-442.

Zhang, H., Lu, S., Zheng, J., Du, J., Wen, S., Tang, D., & Loh, K. (2014). Molybdenum disulfide (MoS 2) as a broadband saturable absorber for ultra-fast photonics. *Optics Express, 22*(6), 7249-7260.

Zhang, H., Lu, S. B., Zheng, J., Du, J., Wen, S. C., Tang, D. Y., & Loh, K. P. (2014). Molybdenum disulfide (MoS(2)) as a broadband saturable absorber for ultra-fast photonics. *Opt Express, 22*(6), 7249-7260. doi:10.1364/OE.22.007249

Zhang, J., Malicka, J., Gryczynski, I., & Lakowicz, J. R. (2005). Surface-enhanced fluorescence of fluorescein-labeled oligonucleotides capped on silver nanoparticles. *The journal of physical chemistry. B, 109*(16), 7643.

Zhang, L. Q., Zhuo, Z., Wang, J. X., & Wang, Y. Z. (2011). Passively Q-switched fiber laser based on graphene saturable absorber. *Laser Physics, 22*(2), 433-436. doi:10.1134/s1054660x12020284

Zhang, M., Howe, R. C. T., Woodward, R. I., Kelleher, E. J. R., Torrisi, F., Hu, G., . . . Hasan, T. (2015). Solution processed MoS2-PVA composite for sub-bandgap mode-locking of a wideband tunable ultrafast Er:fiber laser. *Nano Research, 8*(5), 1522-1534. doi:10.1007/s12274-014-0637-2

Zhao, C., Zhang, H., Qi, X., Chen, Y., Wang, Z., Wen, S., & Tang, D. (2012). Ultra-short pulse generation by a topological insulator based saturable absorber. *Applied Physics Letters, 101*(21), 211106.

Zhou, D.-P., Wei, L., Dong, B., & Liu, W.-K. (2010). Tunable passively $ Q $-switched erbium-doped fiber laser with carbon nanotubes as a saturable absorber. *IEEE Photonics Technology Letters, 22*(1), 9-11.

Zhou, D.-P., Wei, L., & Liu, W.-K. (2012). Tunable graphene Q-switched erbium-doped fiber laser with suppressed self-mode locking effect. *Applied Optics, 51*(14), 2554-2558.

Zhu, J.-J., Liao, X.-H., Zhao, X.-N., & Chen, H.-Y. (2001). Preparation of silver nanorods by electrochemical methods. *Materials Letters, 49*(2), 91-95.

Zhu, W., Qian, L., & Helmy, A. S. (2015). *Implementation of three functional devices using erbium-doped fibers: an advanced photonics lab*.

Zulkifli, A. Z. (2015). *Fabrication and characterisation of graphene oxide saturable absorber for Q-Switched fiber laser generation/Ahmad Zarif bin Zulkifli.* University of Malaya.

LIST OF PUBLICATION

1) Ahmad, H., **Ruslan, N. E**., Ismail, M. A., Reduan, S. A., Lee, C. S. J., Sathiyan, S., ... & Harun, S. W. (2016). Passively Q-switched erbium-doped fiber laser at C-band region based on WS 2 saturable absorber. Applied optics, 55(5), 1001-1005.

2) Ahmad, H., **Ruslan, N. E**., Ali, Z. A., Reduan, S. A., Lee, C. S. J., Shaharuddin, R. A., ... & Ismail, M. A. (2016). Ag-nanoparticle as a Q switched device for tunable C-band fiber laser. Optics Communications, 381, 85-90.

3) Ahmad, H., **Ruslan, N. E**., Ismail, M. A., Ali, Z. A., Reduan, S. A., Lee, C. S. J., & Harun, S. W. (2016). Silver nanoparticle-film based saturable absorber for passively Q-switched erbium-doped fiber laser (EDFL) in ring cavity configuration. Laser Physics, 26(9), 095103.

4) Ahmad, H., Reduan, S. A., Ali, Z. A., Ismail, M. A., **Ruslan, N. E.**, Lee, C. S. J., ... & Harun, S. W. (2016). C-Band Q-Switched Fiber Laser Using Titanium Dioxide (TiO 2) As Saturable Absorber. IEEE Photonics Journal, 8(1), 1-7.

5) Ahmad, H., Lee, C. S. J., Ismail, M. A., Ali, Z. A., Reduan, S. A., **Ruslan, N. E**., ... & Harun, S. W. (2016). Zinc oxide (ZnO) nanoparticles as saturable absorber in passively Q-switched fiber laser. Optics Communications, 381, 72-76.

6) Ahmad, H., Lee, C. S. J., Ismail, M. A., Ali, Z. A., Reduan, S. A., **Ruslan, N. E**., & Harun, S. W. (2016). Tunable Q-switched fiber laser using zinc oxide nanoparticles as a saturable absorber. Applied optics, 55(16), 4277-4281.

7) Ahmad, H., Ismail, M. A., Sathiyan, S., Reduan, S. A., **Ruslan, N. E**., Lee, C. S. J., ... & Harun, S. W. (2017). S-band Q-switched fiber laser using MoSe 2 saturable absorber. Optics Communications, 382, 93-98.